The Abdus Salam
International Centre for Theoretical Physics

United Nations
Educational, Scientific
and Cultural Organization

International Atomic
Energy Agency

310/1749-11

ICTP-COST-USNSWP-CAWSES-INAF-INFN
International Advanced School
on
Space Weather
2-19 May 2006

Transionospheric Propagation: Fundamental processes, total electron content, scintillation

Leonard KERSLEY
Professor Emeritus
Institute of Mathematical & Physical Sciences
University of Wales
Penglais
Aberystwyth SY23 2JA
U.K.

Transionospheric Propagation:
Fundamental processes, total electron content, scintillation

Len Kersley

University of Wales
Aberystwyth
UK

International Advanced School of Space Weather
Trieste, Italy
16 May 2006

Transionospheric Propagation

- Earth / space communication

Outline – Lecture 1

- Introduction
  - Ionosphere
  - Radio propagation – magneto-ionic theory
- Effects of bulk ionosphere
  - Total electron content (TEC)
- Effects of small-scale irregularities
  - Scintillation

Prifysgol Cymru Aberystwyth The University of Wales

Transionospheric Propagation

- Earth / space communication

Outline – Lecture 2

- Radio tomography
  - Ionospheric imaging
- Effects of space weather
  - High-latitude ionosphere

Prifysgol Cymru Aberystwyth The University of Wales

Ionospheric Basics

- Vertical profiles of electron density
  N versus h
- Variable structure – vert. and hor.
- Interaction of basic mechanisms

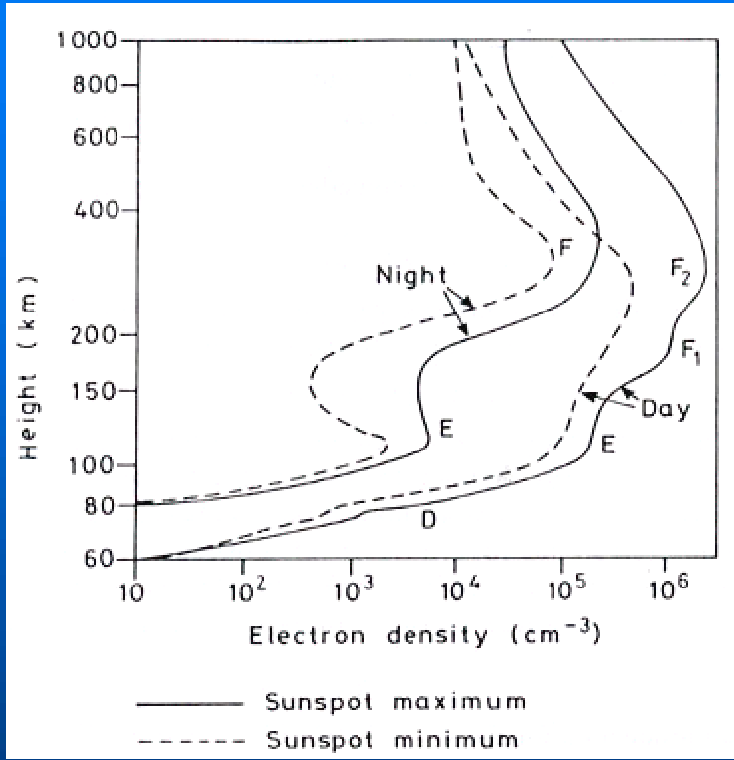

Continuity equation

$$\Delta N/\Delta t = q - L - \mathrm{div}(N\mathbf{v})$$

Electron density rate change

Production

Loss

Transport

Ionospheric Basics - Production

- Production (q)
  - solar euv radiation
    - atomic oxygen (O^+) plasma in F2-layer
  - particle precipitation
    - impact ionisation
    - high latitudes
    - ionospheric storms

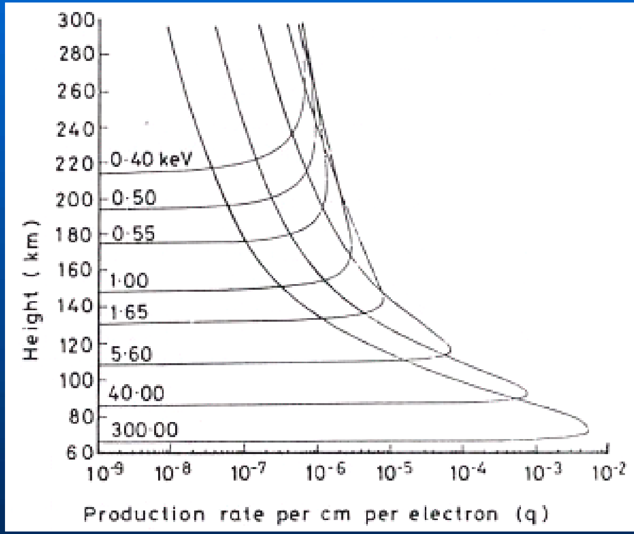

Ionospheric Basics - Loss

- Loss (L)
  - neutral atmosphere chemistry
    - molecular species (N_2)
    - reaction rates
      - temperature dependent
      - velocity dependent
  - composition changes
    - $[O] / [N_2]$ ratio
    - production / loss processes
    - storms

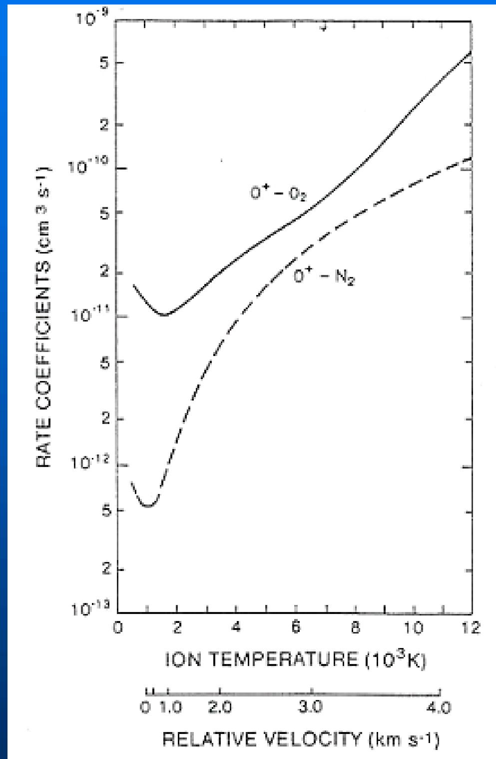

Ionospheric Basics - Transport

- Transport div(N**v**)
  - motion constrained by magnetic field
    - neutral winds
      - diurnal, seasonal, storm
    - diffusion
      - $O^+ \leftrightarrow H^+$ protonosphere
- electric fields - **E**x**B** convection
  - equatorial anomaly
  - high latitudes

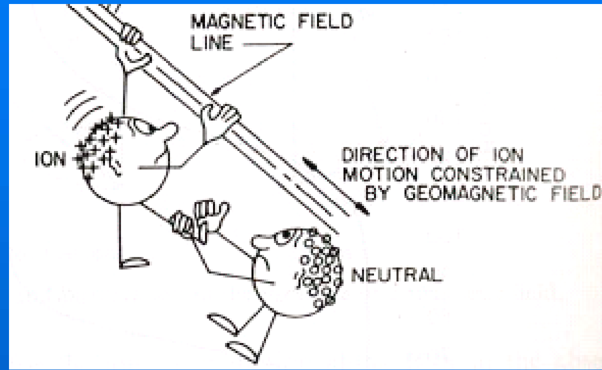

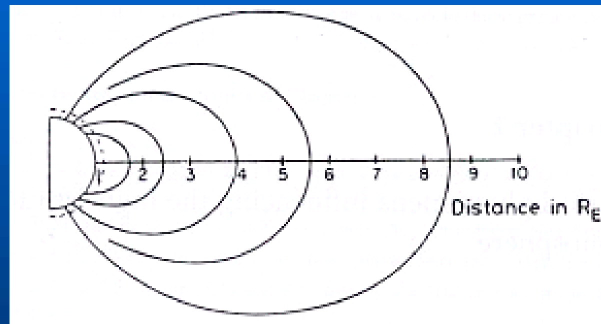

Prifysgol Cymru Aberystwyth The University of Wales

Ionospheric Structure

- Electron density at any place and time depends on the *balance* between *many different processes*
- Ionosphere has *temporal* variability on many scales
  - solar cycle, seasonal, diurnal, etc
- Ionosphere is structured *spatially* on many different scales
  - from geographic (hundreds of kilometres) to small-scale irregularities (metres)
- *F2-region* of ionosphere is responsible for most of the effects on *transionospheric* radio signals
  - 2/3 of electrons are above F2 peak

Prifysgol Cymru Aberystwyth The University of Wales

Plasma Basics – Plasma Frequency

- Plasma frequency (ω_N)

  Natural oscillation frequency of electrons in a plasma

  $$\omega_N = (N e^2 / \varepsilon_o m_e)^{1/2}$$

  $$\text{or } f_N = (80.6\, N)^{1/2} \text{ when } N \text{ is in } m^{-3} \text{ and } f_N \text{ in Hz}$$

- Non-dimensional form of plasma frequency (X)

  For a radio wave of frequency (ω) propagating in a plasma it is useful to express the plasma frequency squared in a non-dimensional form

  $$X = (\omega_N / \omega)^2 = (N e^2 / \varepsilon_o m_e \omega^2)$$

Reflection of a radio wave in a plasma

- Reflection

Radio wave of frequency *(ω)* is reflected in a plasma at vertical incidence when

$$\omega = \omega_N$$

that is, at the particular height level with the appropriate electron density

- Transionospheric propagation

For radio wave to pass through ionosphere without reflection

- need $\omega > \omega_N$ at vertical incidence
- and $\omega >> \omega_N$ at oblique incidence

so only *vhf and higher frequencies* will cross the ionosphere

Prifysgol Cymru Aberystwyth The University of Wales

Plasma Basics -Gyrofrequency

- Gyrofrequency (ω_B)

  Gyration frequency of electrons about a magnetic field

  $$\omega_B = B\, e / m_e \qquad\qquad or\ f_B = B\, e / 2\pi\, m_e$$

  - for Earth's magnetic field B ~ 0.5 T then f_B ~ 1.4 MHz

- Non-dimensional form of gyrofrequency (Y)

  For a radio wave of frequency (ω) propagating in a plasma
  it is useful to express the gyrofrequency in a non-dimensional form

  $$Y = \omega_B / \omega = B\, e / m_e\omega$$

- Often useful to treat gyrofrequency in terms of components *along* (Y_L) and *transverse* to the magnetic field (Y_T)

  For many transionospheric situations the propagation can often to considered to be *quasi-longitudinal* so that Y_T can be neglected

Basic Magneto-ionic Theory

How is radio wave affected by ionosphere?
Need *refractive index* for propagation of radio wave in ionosphere

Appleton Equation (Appleton-Hartree Equation)

$$n^2 = 1 - \frac{X}{1 - jZ - \frac{Y_T^2}{2(1 - X - jZ)} \pm \left(\frac{Y_T^4}{4(1 - X - jZ)^2} + Y_L^2 \right)^{1/2}}$$

'It is virtually impossible for an ordinary mortal to make much sense of the Appleton equation(s) in their full glory.'

(Hunsucker and Hargreaves, 2003)

Appleton Equation

$$n^2 = 1 - \frac{X}{1 - jZ - \frac{Y_T^2}{2(1-X-jZ)} \pm \left(\frac{Y_T^4}{4(1-X-jZ)^2} + Y_L^2 \right)^{1/2}}$$

- $X = (\omega_N / \omega)^2$
  where $\omega_N = (Ne^2 / \varepsilon_o m_e)^{1/2}$ is *plasma frequency*
  X depends on *electron density (N)*

- $Y = \omega_B / \omega$
  where $\omega_B = Be / m_e$ is *electron gyrofrequency*
  Y depends on *magnetic field (B)*

- $Z = v / \omega$
  Z depends on the *electron collision frequency (v)*

- Refractive index (n) of an ionised medium with electron density (N), a magnetic flux (B) and electron collision frequency (*v*)

Appleton Equation (cont)

$$n^2 = 1 - \frac{X}{1 - jZ - \frac{Y_T^2}{2(1 - X - jZ)} \pm \left(\frac{Y_T^4}{4(1 - X - jZ)^2} + Y_L^2 \right)^{1/2}}$$

- $n = \mu - j\chi$ is *complex*,
  - *real* part - *phase propagation*
  - *imaginary* part - *absorption of wave*
    - Z non-dimensional collision frequency
- ± signs correspond to *ordinary* and *extraordinary* waves
- Y has components *along* (Y_L) and *transverse* (Y_T) to the magnetic field

Fortunately, for most applications approximations can be used that reduce the Appleton equation to very much simpler forms

Appleton Equation – Useful Approximations for Transionospheric Propagation

- $Z = 0$ - since collisions are only important in the lower ionosphere (D-layer) where the neutral density is high
- $Y = 0$ - effects of magnetic field can *often* be neglected because radio frequency >> gyrofrequency $(\omega >> \omega_B)$
- $Y_T = 0$ - even when magnetic field is included in most circumstances only the component in the propagation direction (Y_L) needs to be considered
- $\omega >> \omega_N$ - for transionospheric propagation the radio frequency must be very much greater than the maximum plasma frequency encountered (*foF2)*

Prifysgol Cymru Aberystwyth The University of Wales

Appleton Equation – No Magnetic Field

Neglecting the magnetic field *(Y=0)* and collisions *(Z=0)*

$$n = (1 - X)^{1/2} = \{1 - (\omega_N / \omega)^2\}^{1/2} = \{1 - N e^2 / \varepsilon_o m_e \omega^2\}^{1/2}$$

For transionospheric signals with $\omega >> \omega_N$ can expand binomially and neglect higher order terms so that the refractive index

$$n = 1 - X/2 = 1 - N e^2 / 2\varepsilon_o m_e \omega^2 = 1 - 40.3\, N / f^2$$

(with N in m^{-3} and f in Hz)

While $n = 1 - X/2$ is the approximation currently used for most transionospheric propagation applications, it must be noted that for super-resolution (< 2cm error) use of GPS positioning consideration of higher-order terms involving the magnetic field is becoming of interest

Phase velocity of radio wave

The phase velocity of the radio wave will be given by

$$v_p = c / n = c / (1 - N e^2 / 2\varepsilon_o m_e \omega^2)$$

- phase velocity > c
- phase of carrier wave will advance wrt free space
- Doppler shift in frequency

Consider a radio wave of frequency *(f)* and wavelength *(λ)* propagating along a path *(l)* through the ionosphere:

Carrier Phase Advance and Doppler Shift

After travelling a distance *dl* (ie dl/λ wavelengths) *phase of the wave* has changed by

$$2\pi\, dl/\lambda = 2\pi f\, n\, dl / c$$

Thus over a path *l* through the ionosphere the *phase change* will be

$$-(2\pi f / c) \int n\, dl / c = - 2\pi f\ l / c\ + (2\pi\ x\ 40.3 / cf) \int N\, dl$$

Change in phase of a wave travelling at the speed of light

Phase *advance* due to the *medium*

- phase advance is *cumulative* along path
- depends on the *Total Electron Content (TEC)* along slant path

$$N_T = \int N\, dl$$

Numerically, *phase advance* (in radians) due to the ionosphere is

$$\varphi = (8.45\ x\ 10^{-7})\, N_T / f \qquad \text{(with } N_T \text{ in } m^{-2} \text{ and } f \text{ in } Hz\text{)}$$

Since *frequency* is *rate of change of phase*, ionosphere imposes *Doppler shift* on the wave

Group Propagation

Group propagation – group refractive index (n_g)

$$n_g = c / u = c\,(\partial k/\partial \omega) = c\,(\partial (n\omega)/\partial \omega) = c(n + \omega\,(\partial n/\partial \omega))$$

Group velocity (u)

$$u = c / n_g = c\,(1 - N e^2 / \varepsilon_o m_e \omega^2)^{1/2}$$

- group velocity $(u) < c$
- group delay of modulation phase
- time delay of pulse

Group Delay and Time Delay

If carrier wave of frequency f is modulated at a frequency f_m the phase of the modulation is *retarded* by

$$\varphi_m = -8.45 \times 10^{-7} (f_m / f^2) N_T$$

There is a *group delay* because the modulation travels at the group velocity *(u<c)*

Hence, there is a *time delay* of a pulse

$$\Delta t = -(8.45 \times 10^{-7} / 2\pi f^2) N_T$$

Both *group and time delays* depend directly on
Total Electron Content (*TEC*) – line integral of electron density along the ray path $N_T = \int N \, dl$

Prifysgol Cymru Aberystwyth The University of Wales

Ionospheric Time Delay

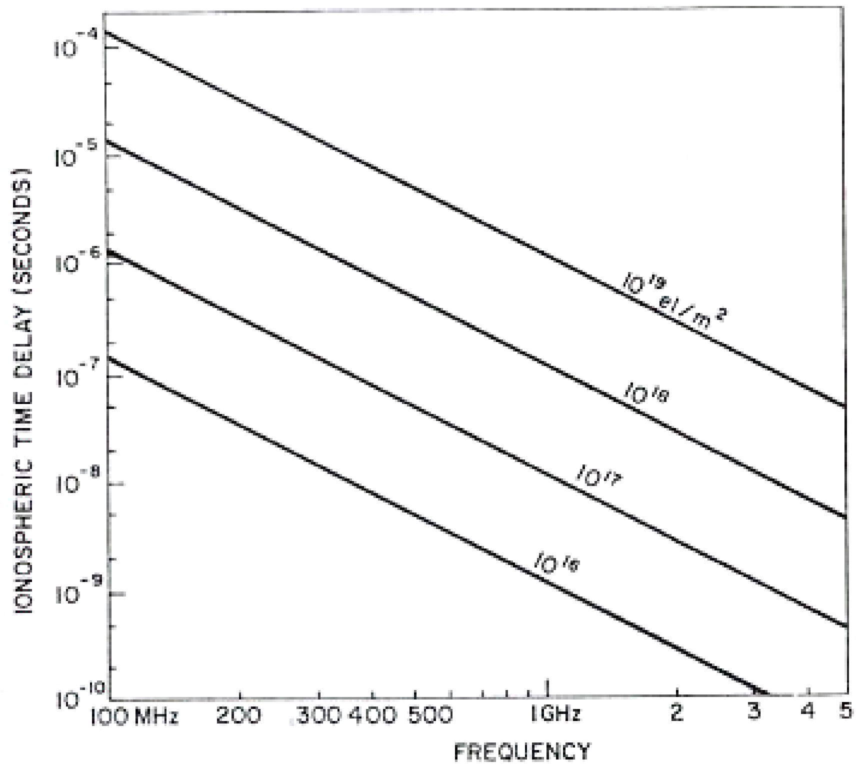

Fig. 8.19 *Excess time delay versus frequency for several TECs (From Klobuchar 1978, with permission)*

Appleton Equation – Magnetic Field

Effect of magnetic field

$$n^2 = 1 - X / (1 \pm Y_L)$$

or $n = 1 - ½ X \pm ½ XY_L$ for transionospheric propagation

- field component in propagation direction
- longitudinal approximation - Y_L only
- ± ordinary and extraordinary waves
- o and e waves travel at different speeds
- leads to polarisation (Faraday) rotation
- $n_O - n_E = XY_L$ if radio frequency (f) >> gyrofrequency (f_B)

Prifysgol Cymru Aberystwyth The University of Wales

Faraday Effect – Polarisation Rotation

When geomagnetic field is taken into account the propagation comprises *ordinary and extraordinary* waves - circularly polarised in opposite directions

If θ_O and θ_E are the respective instantaneous angles of the ordinary and extraordinary components, these combine to give a linearly polarised wave at an angle

$$\Omega = (\theta_O + \theta_E) / 2$$

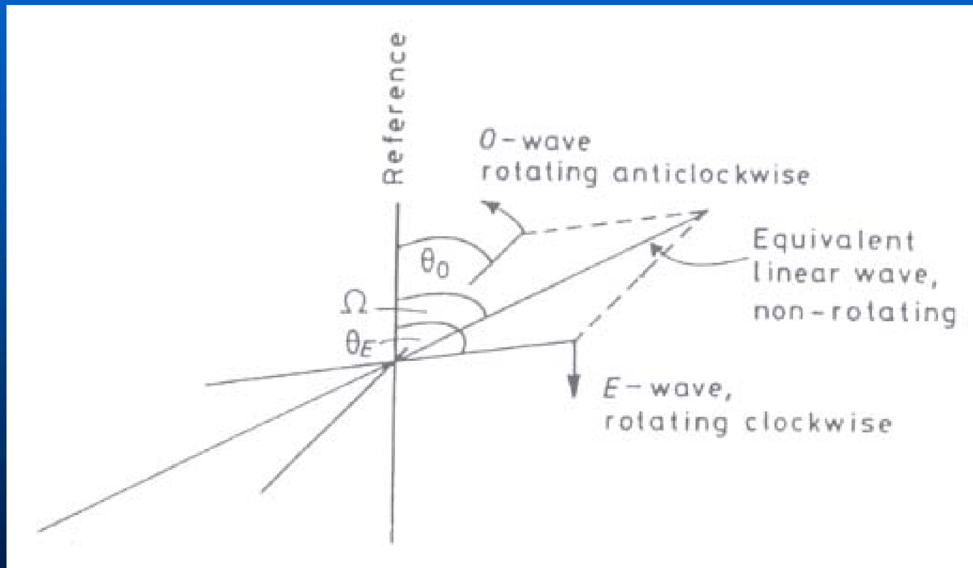

Faraday Rotation (continued)

Ordinary and extraordinary waves have different refractive indices and travel at different speeds, so after distance *dl* in the medium the polarisation of resultant wave will have rotated by

$$d\Omega = (\pi f / c)\,(n_O - n_E)\,dl = (\pi f / c)\,XY_L\,dl = (\pi f / c)\,((f_N)^2 f_L / f^3)\,dl$$

Thus for a path through the ionosphere where both the electron density and the magnetic field vary, the polarisation rotation will be

$$\Omega = (8.45 \times 10^{-7} / f^2) \int f_L\,N\,dl = (2.36 \times 10^4 / f^2) \int B_L\,N\,dl$$

where B_L is the component of magnetic field in the propagation direction

If an appropriate mean value of B_L can be assumed then

$$\Omega = 2.36 \times 10^4 \langle B_L \rangle / f^2) \int N\,dl = 2.36 \times 10^4 \langle B_L \rangle / f^2)\,N_T$$

that is *Faraday rotation* depends on *TEC*

Prifysgol Cymru Aberystwyth The University of Wales

Ionospheric Faraday Rotation

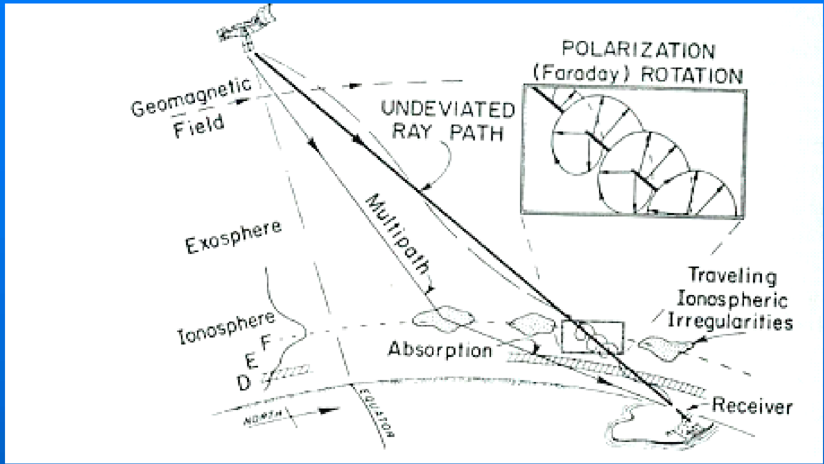

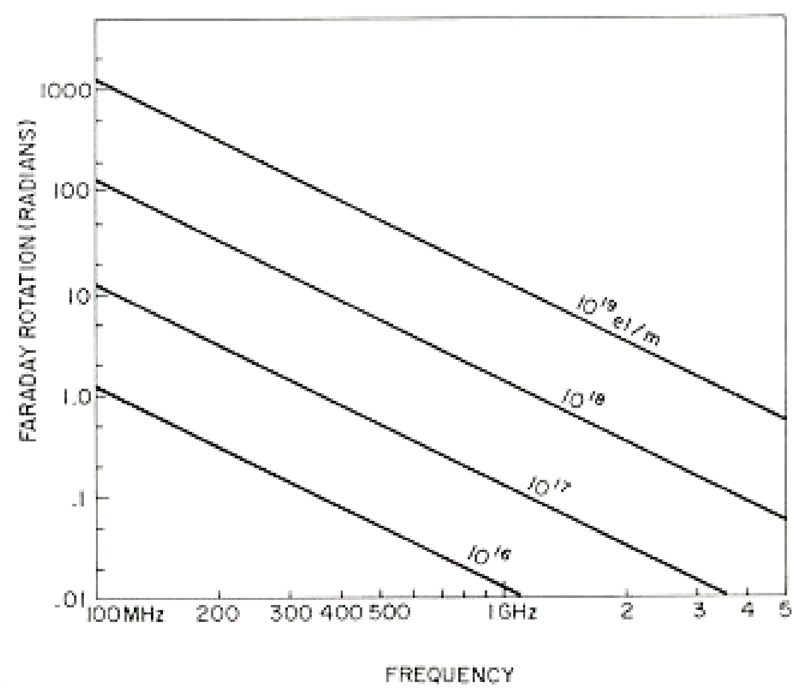

Fig. 8.18 *Approximate Faraday rotation as a function of frequency and TEC for a ray path in a magnetic meridian (From Klobuchar 1978, with permission)*

For particular station and geometry ie mean B_L

Importance of Total Electron Content

For a radio wave crossing the ionosphere

- Carrier phase advance
- Group delay
- Faraday rotation
- Refraction

all depend on

- Total Electron Content (TEC)
- line integral of electron density along ray path
- $N_T = \int N\, dl$

Prifysgol Cymru Aberystwyth The University of Wales

Practical Significance of TEC

Radio systems using signals from satellites or natural sources that cross the ionosphere will be subject to errors due to the line integral of the electron density, that is, the *total electron content (TEC)* along the ray path

Applications include:

- Navigation
- Positioning
- Time transfer
- Radar
- Radio astronomy

Mitigation of the effects requires measurement or modelling of TEC

Prifysgol Cymru Aberystwyth The University of Wales

Total Electron Content (TEC) –some definitions

- *Slant total electron content* $N_T = \int N\, dl$
  - TEC along slant ray path *l*

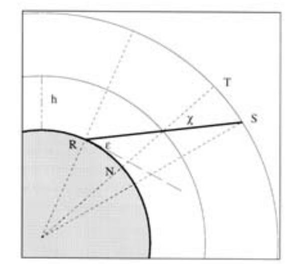

Figure 4.2. Diagram showing conversion from slant (R-S) to vertical (N-T) TEC for an elevation angle ε and satellite zenith angle χ.

- *Vertical total electron content* $N_T = \int N\, dh$
  - measure using incoherent scatter radar
  - integrate through tomographic image
- *Equivalent vertical electron content*
  - assume thin-layer ionosphere at chosen height
  - simple geometrical mapping function $dl = dh \sec\chi$
  - usually what is meant by TEC
- *Faraday electron content*
  - assume mean magnetic field ($\langle B_L \rangle$)
  - upper limit usually taken ~ 2000 km

Prifysgol Cymru
Aberystwyth
The University of Wales

Measurement of total electron content (TEC)

- Faraday rotation
  - Early measurements
  - Geostationary satellites
  - Diurnal variations
  - TEC morphology
- Differential carrier phase (differential doppler)
  - NNSS or NIMS satellites in low Earth orbit
  - TEC versus latitude
  - Radio tomography
- Combinations of techniques
  - Protonospheric content
  - GPS - phase and code measurements
- TEC Units
  - 1 TECU = 10^{16} m^{-2}

Prifysgol Cymru Aberystwyth The University of Wales

Mid-latitude TEC – temporal variations

Diurnal TEC plots from geostationary satellite Faraday rotation of radio signals at about 136MHz

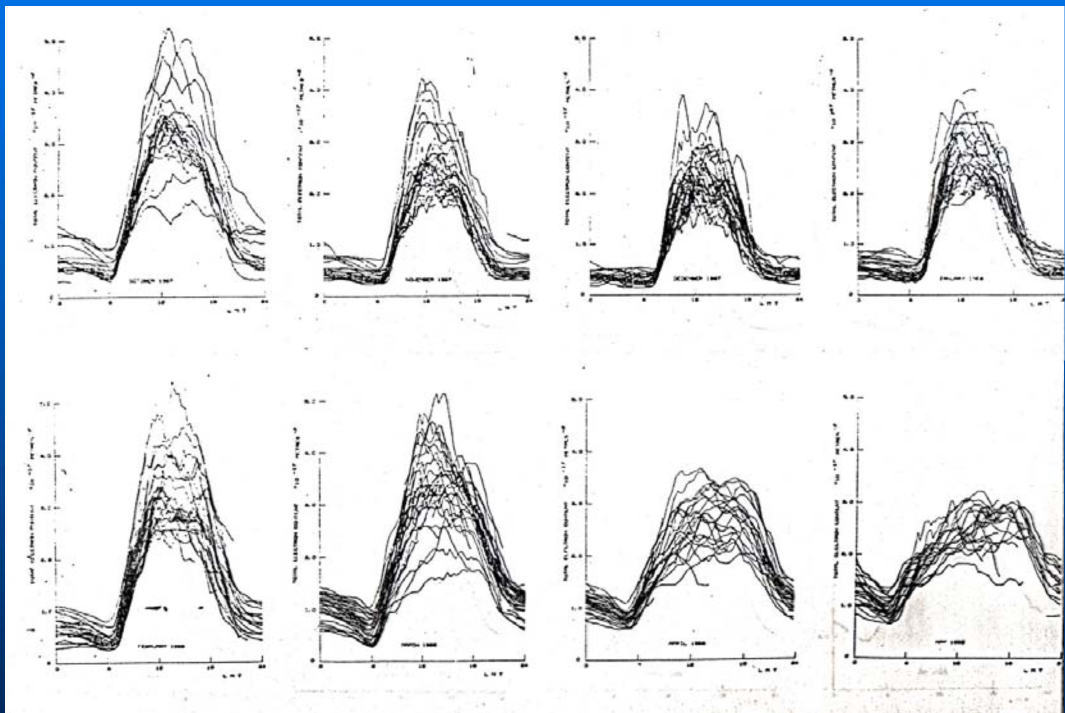

Aberystwyth 52^{o} N   Europe

- Daytime maximum
- Low nighttime values
- Equinox maximum
- Summer daytime bite-out
- Day-to-day variability

Prifysgol Cymru
Aberystwyth
The University of Wales

Mid-latitude TEC - temporal variations

Diurnal TEC plots from geostationary satellite Faraday rotation

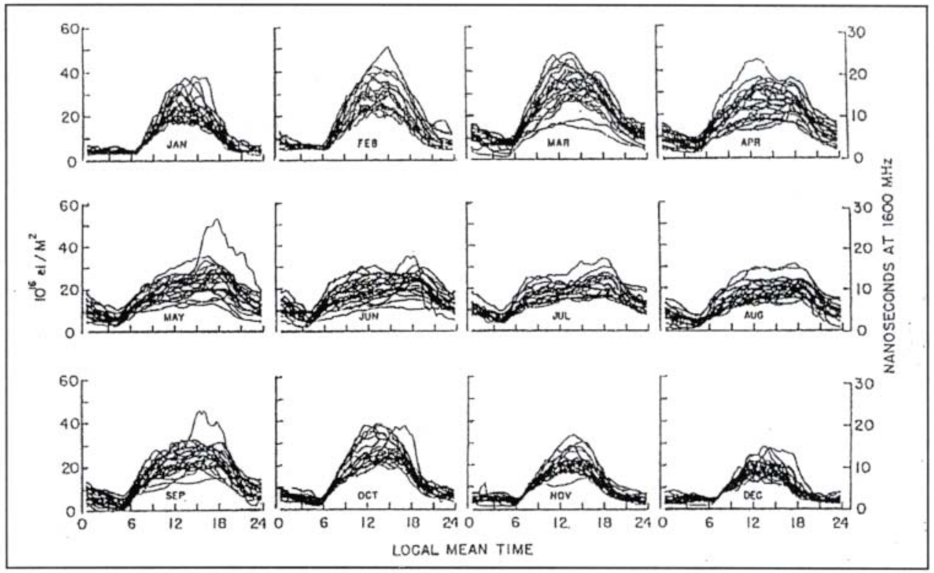

Figure 2.2. Equivalent vertical total electron content, in over-plot format, from observations of ATS-3 made at the Sagamore Hill Radio Observatory, Hamilton, Massachusetts, in 1972 (Mendillo and Klobuchar, 1974).

Hamilton 42^o N   USA

- Daytime maximum
- Nighttime decline
- Equinox maximum
- Low summer daytime
- Day-to-day variability

Prifysgol Cymru Aberystwyth The University of Wales

TEC Variability
Percentage Standard Deviations

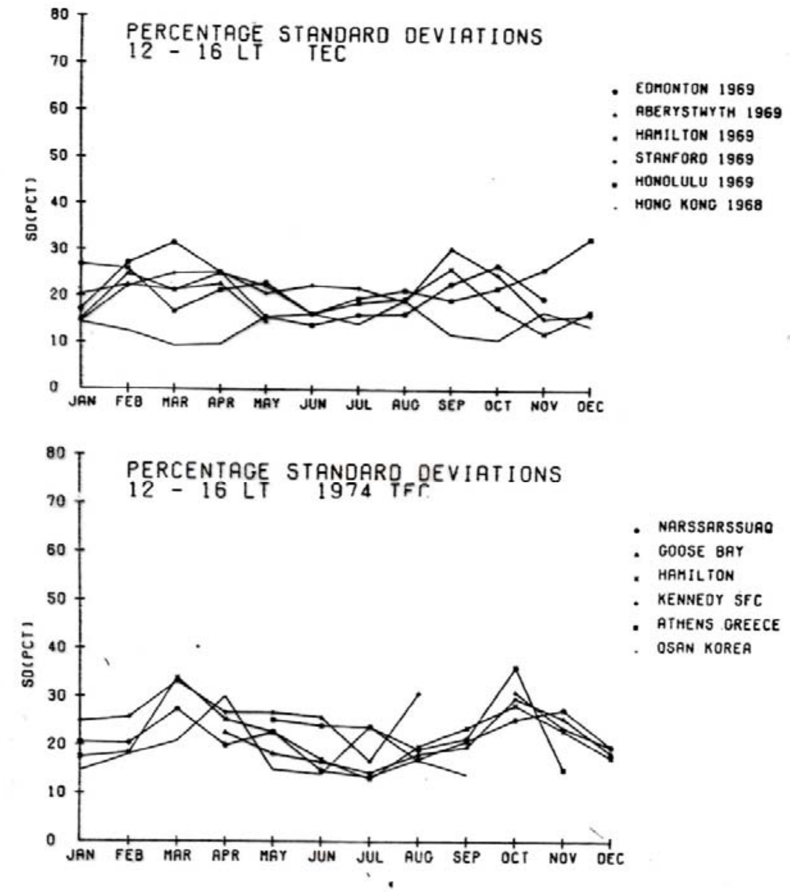

Fig. 5. Daytime percentage standard deviation vs. month for solar maximum and solar minimum conditions.

- Day-to day variability
- Standard deviations ~ 25%

Mid-latitude TEC and Solar Activity

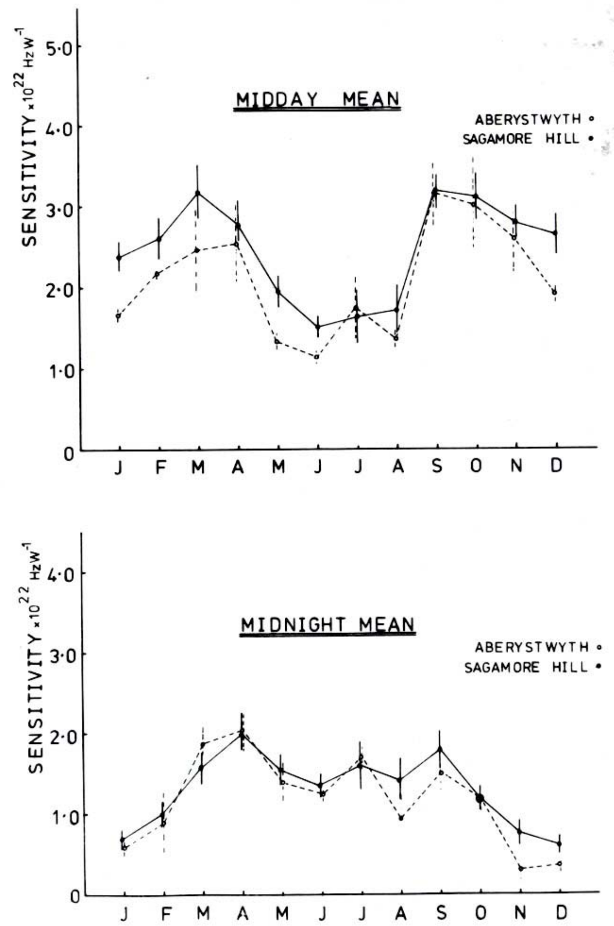

FIG. 1. Sensitivity of total electron content ($\times 10^{-15}$ m^{-2}) response to solar flux as a function of calendar month.

$$\mathrm{TEC} = \mathrm{TEC}(80) + a(\overline{S} - 80) \times 10^{15}\ \mathrm{m}^{-2}$$

where $\mathrm{TEC}(80)$ = total electron content at $80 \times 10^{-22}\ \mathrm{W m^{-2} Hz^{-1}}$

a = sensitivity of TEC to change in solar flux

and $\overline{S}$ = monthly mean solar flux at 10.7 cm.

- Seasonal dependence during daytime
- Latitudinal dependence in winter
- Highest TECs are found at the equatorial anomaly latitudes at solar maximum

Prifysgol Cymru Aberystwyth The University of Wales

NIMS Satellites - spatial TEC gradients

- NIMS – Navy Ionospheric Monitoring Satellites
- up to six satellites, formerly NNSS
- circular polar orbits at 1100 km altitude

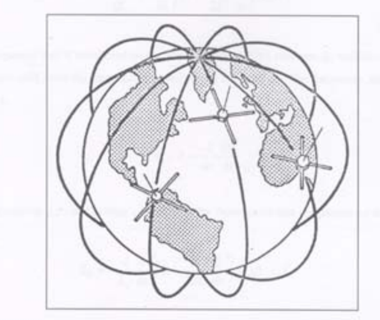

Figure 3.2. The NNSS satellite constellation (Ashkenazi et al. 1977).

- coherent transmissions at 150 MHz and 400 MHz
- differential carrier phase (differential Doppler) technique
- measure total electron content along ray paths
- TEC as a function of latitude

Prifysgol Cymru Aberystwyth The University of Wales

Differential Carrier Phase (Differential Doppler) Technique

Satellite transmits two *coherent* frequencies *f* and *pf,* where p is constant (NIMS satellites transmit on 150MHz and 400MHz so that $p = 8/3$)

Compare *received phase of lower frequency* with that of the *higher frequency divided by p*

$$\Delta\varphi = \varphi_f - \varphi_{pf} = \{-2\pi f\, l/c + 2\pi\, x40.3\, N_T / f\, c\} - \{(1/p)(\{-2\pi\, p\, f\, l/c + 2\pi\, x40.3\, N_T / pf\, c\}$$

The *first and third terms cancel* because they represent the phase changes for *free space propagation* of the two signals along the path

Thus the *differential phase shift* due to the ionospheric TEC is

$$\Delta\varphi = \{1 - 1/p^2)\,(8.45 \times 10^{-7})\, N_T / f$$

Can measure *relative phase accurately* but still have 2π ambiguity to solve to get *absolute TEC*

Prifysgol Cymru Aberystwyth The University of Wales

Absolute TEC from Differential Carrier Phase Measurements

- With two or more stations separated in latitude can match the observation in the region of overlap to give the same equivalent vertical TEC

- Hence obtain *absolute* TEC measurements versus latitude

Equivalent Vertical TEC

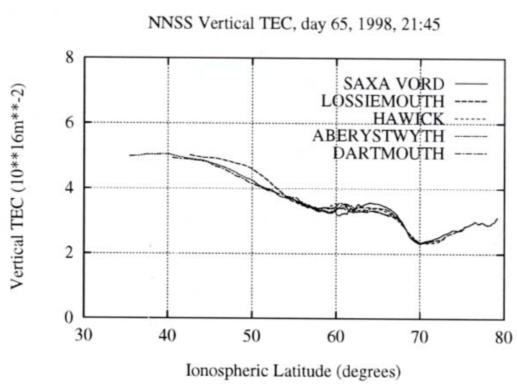

Figure 4.4. Equivalent Vertical TEC obtained from the multi-station method from NNSS observations at 5 stations in the UK of the satellite pass at 21:45 UT on 6 March 1998.

Latitude

Importance of NIMS TEC studies

- Latitudinal TEC gradients
- Spatial structure
- Remote regions – polar cap
- Equatorial anomaly region
- Main (mid-latitude) trough
- Radio tomography

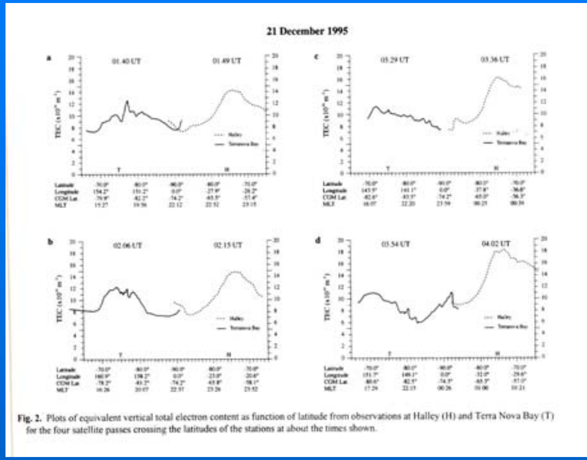

TEC across Antarctica

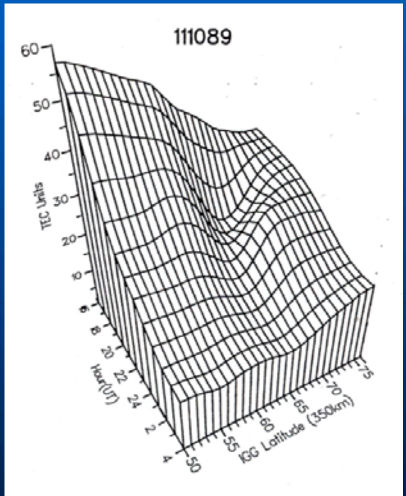

TEC in main trough

GPS Satellites

- > 24 satellites in 6 orbital planes
- circular orbits at 55^{o} inclination
- 20200 km altitude
- 12 siderial hours period
- same track 237 s earlier each day
- L1 frequency 1575.42 MHz
- L2 frequency 1227.60 MHz
- pseudo random noise (PRN) modulation
- coarse acquisition (C/A) code on L1 carrier
- precision (p) code on both L1 and L2
- receiver uses PRN code to estimate travel time of signal
- calculate distance or pseudo-range from satellite
- receiver also determines phase pseudo-range for carrier
- RINEX (receiver independent exchange) data format
- observables – phases, code ranges, Doppler shifts on 2 freqs
- navigation message – orbit parameters

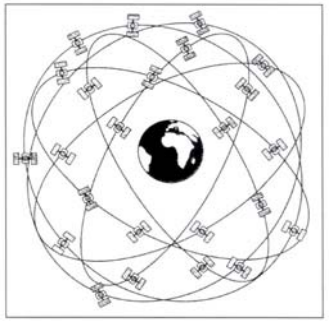

Figure 3.1. The GPS satellite constellation (Hajj et al. 1994).

Prifysgol Cymru Aberystwyth The University of Wales

GPS slant TEC during pass

‘p code pseudo range’
(differential group delay)
measurements

‘phase pseudo range
(differential carrier phase)
measurements

Processing to determine
many bias errors and
find absolute TEC

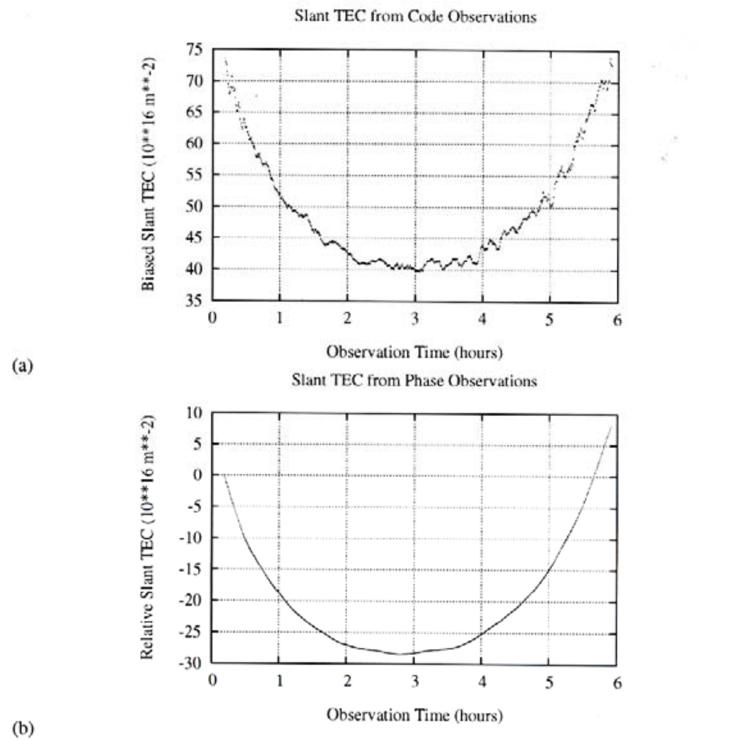

Figure 4.1. (a) Slant TEC measurements derived from p code pseudo-range measurements (the differential group delay measurements) for PRN 05 on the 29 June 1998. (b) Slant TEC derived from the phase pseudo-range measurements (the differential carrier phase measurements) for the same satellite on the same day as in (a). The observations cover the entire satellite pass seen from Aberystwyth.

multipath

Prifysgol Cymru
Aberystwyth
The University of Wales

GPS TEC – diurnal plots

Data from many passes with differing geometries

Processing – eg SCORE

Solve for unknowns to get absolute TEC

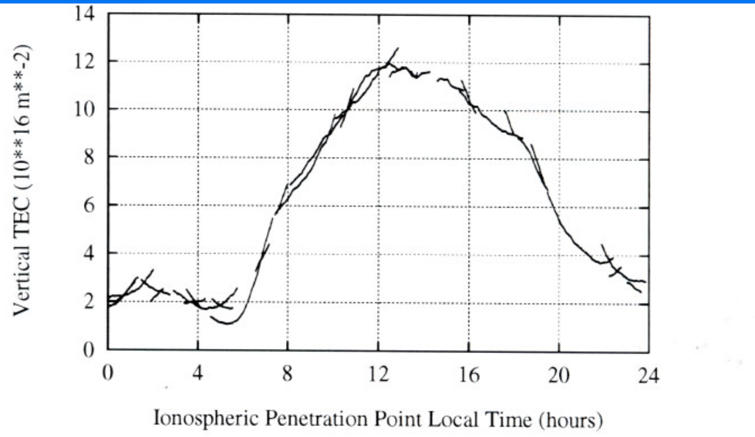

Figure 4.3. Equivalent Vertical TEC obtained from SCORE processed GPS observations on 6 March 1998 for the one degree wide latitude band centred over Aberystwyth.

1 TECU represents a range error of ~ 16 cm for GPS L1 frequency

TEC Maps from GPS

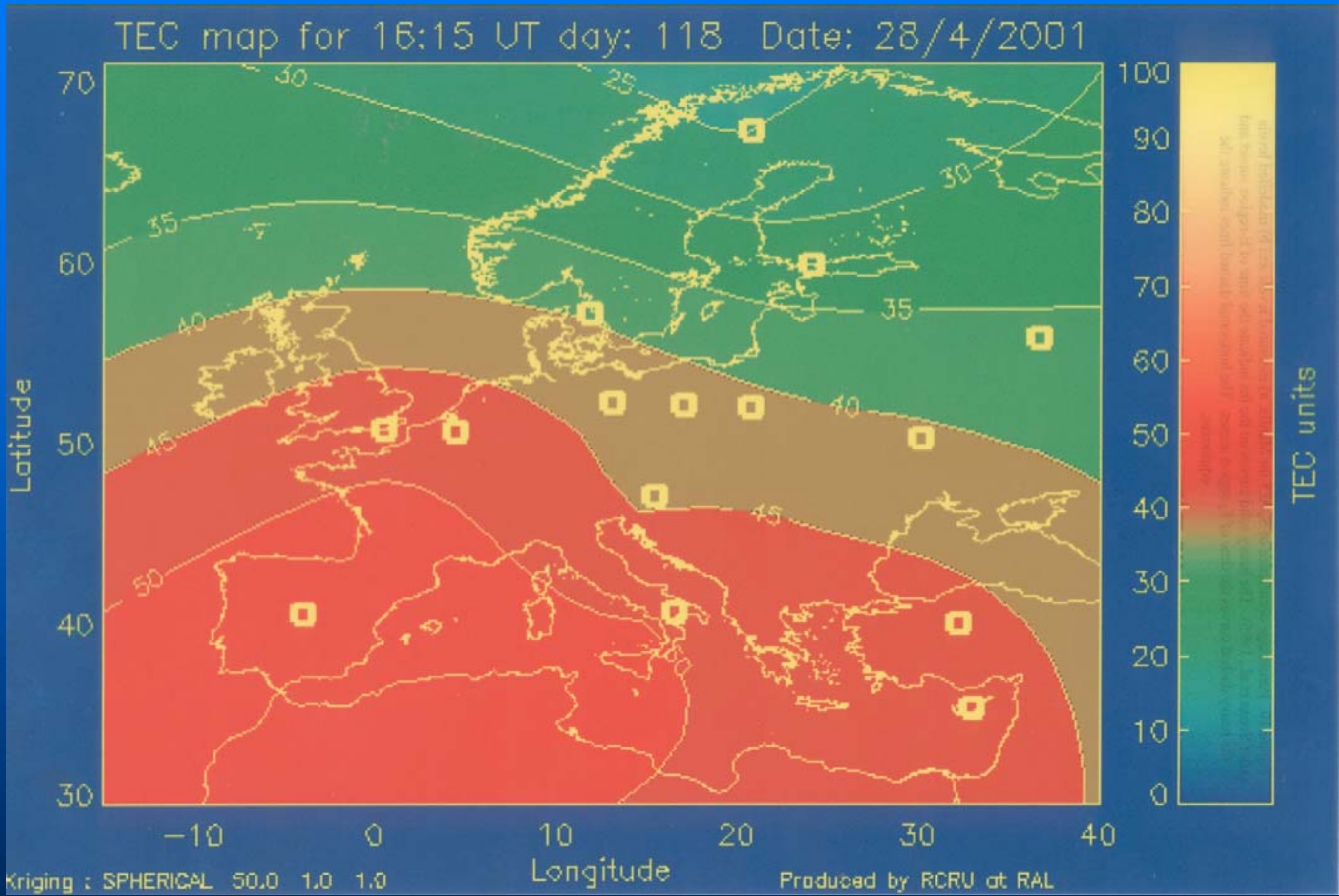

Effects of space weather on mid-latitude TEC - ionospheric storms

- strong enhancements on first day
- sudden collapse
- very steep spatial gradients
- depressed values for several days
- composition changes
- contraction of plasmapause
- storm enhanced densities (SEDs)
- slow refilling of plasmasphere

Prifysgol Cymru Aberystwyth The University of Wales

Mid-latitude TEC during Geomagnetic Storms

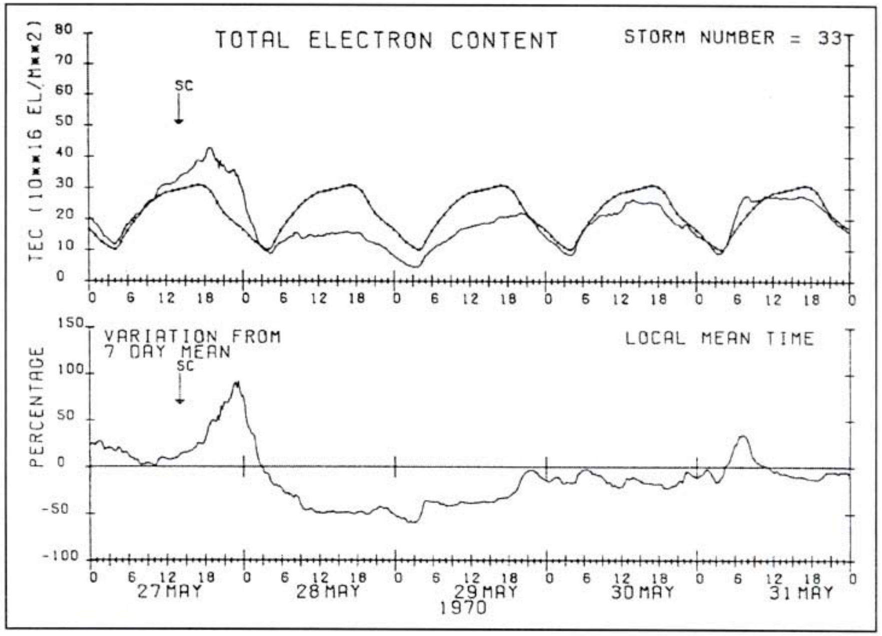

Figure 2.3. The development of an ionospheric storm. The top plot shows the TEC for the first few days of a storm plotted with the mean TEC values of the seven days prior to the commencement of the storm. The lower plot is the difference between the recorded and mean values (Mendillo and Klobuchar, 1974).

- Initial positive phase
- Collapse around 1800 LT on first day of storm
- Depleted TEC for several days subsequently
- Low nighttime values
- Composition changes
- [O] / [N_2] ratio
- Plasmapause contraction

Prifysgol Cymru Aberystwyth The University of Wales

Storm Contraction of Plasmapause

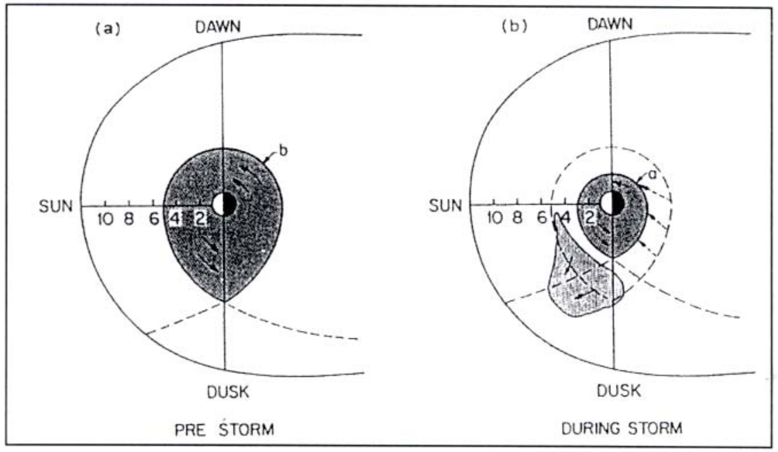

Figure 2.5. Diagram of the plasmasphere, a) quiet period before storm, b) after increased convection has peeled off the outer layers of the region. The grey areas denote high plasma concentrations, filled arrows denote plasma motion, the dotted arrows show the movement of the plasmapause and the scale is in L (Chappell, 1972).

- Can result in very severe spatial gradients in mid-latitude ionosphere - storm enhanced densities (SEDs)
- Problems for GPS applications (eg WAAS & EGNOS)

Protonospheric Content - Flux-Tube Geometry

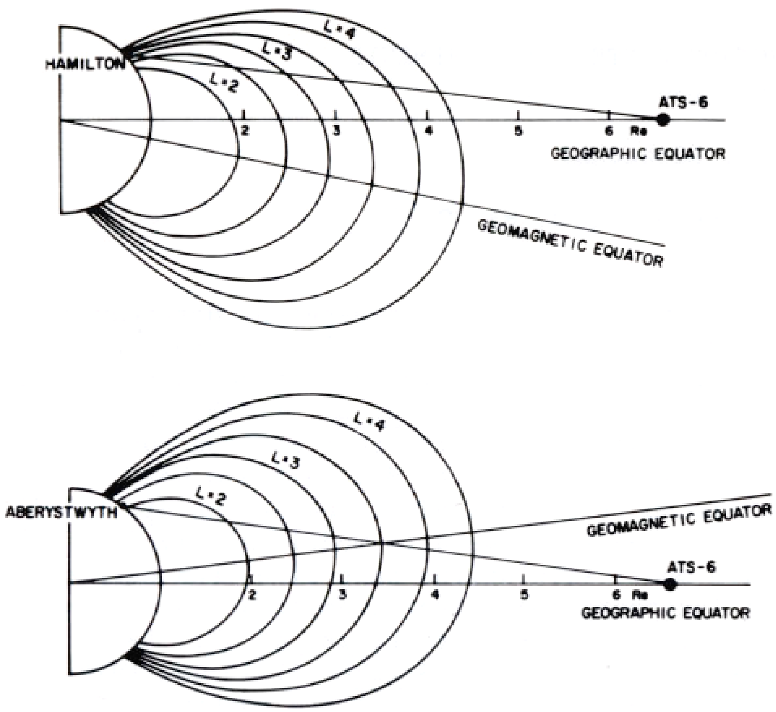

Fig. 1. Geomagnetic field line configurations for ATS-6 ray paths to (a) Hamilton and (b) Aberystwyth.

- Flux tubes replenished by diffusion from ionosphere
- O^+ / H^+ transition
- Flux Tube Volume ~ L^3
- Low L-shells – diurnal exchange with ionosphere
- Higher L-shells – never fill completely between storms

Prifysgol Cymru Aberystwyth The University of Wales

Protonospheric Content
Storm Collapse and Slow Recovery

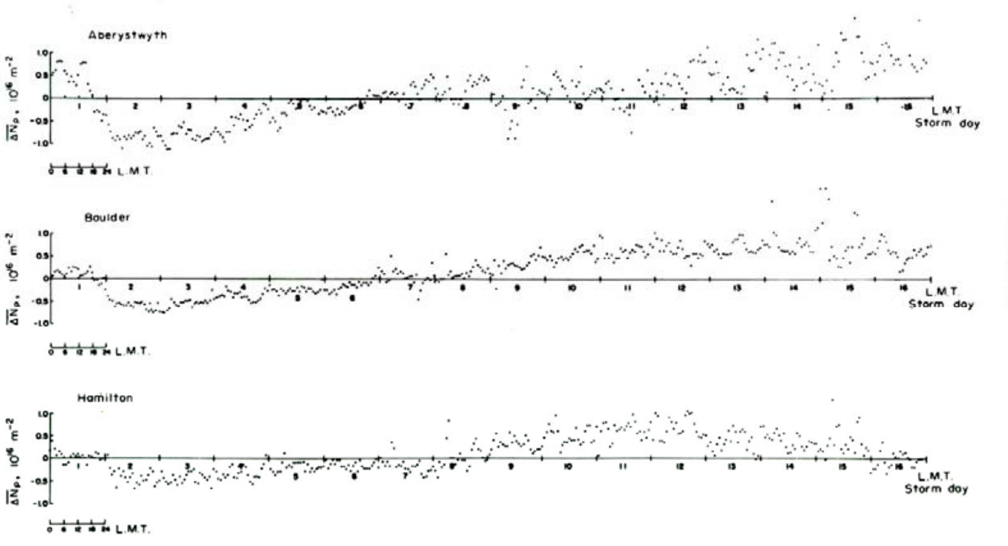

FIG. 3. AVERAGE VARIATION OF HOURLY VALUES OF RESIDUALS FROM CORRESPONDING MONTHLY MEANS OF PROTONOSPHERIC CONTENT PLOTTED IN LOCAL MEAN TIME THROUGHOUT THE STORM AND RECOVERY PERIODS FOR ABERYSTWYTH, BOULDER AND HAMILTON.

- Collapse in evening of storm day
- Slow replenishment over many days

Prifysgol Cymru Aberystwyth The University of Wales

Slab Thickness (τ)

Slab Thickness (τ) = TEC / Maximum Electron Density (NmF2)

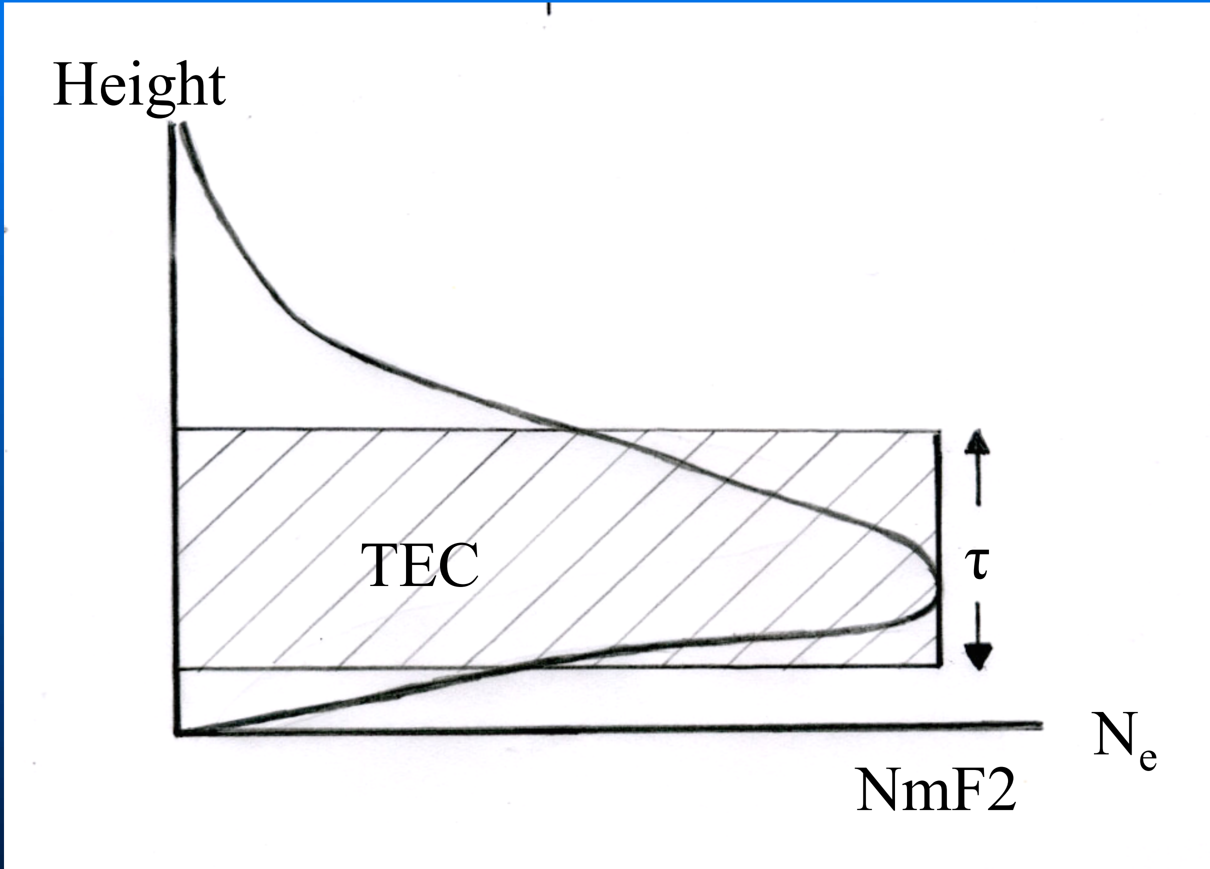

Slab Thickness Variations

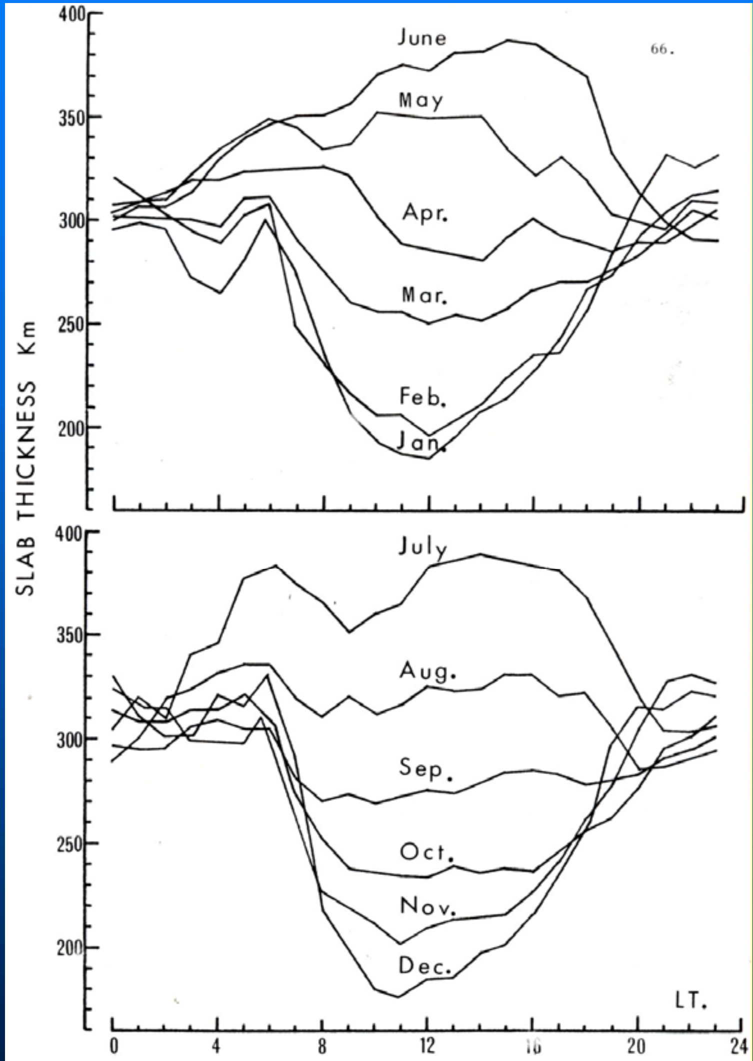

Fig. 4.
Diurnal variations of monthly mean slab thickness at solar maximum (1968 - 1970).

- ~ 300 km at night
- max summer daytime
- min winter daytime

Accuracy of TEC measurements

Problems with layer height assumption in equivalent vertical TEC

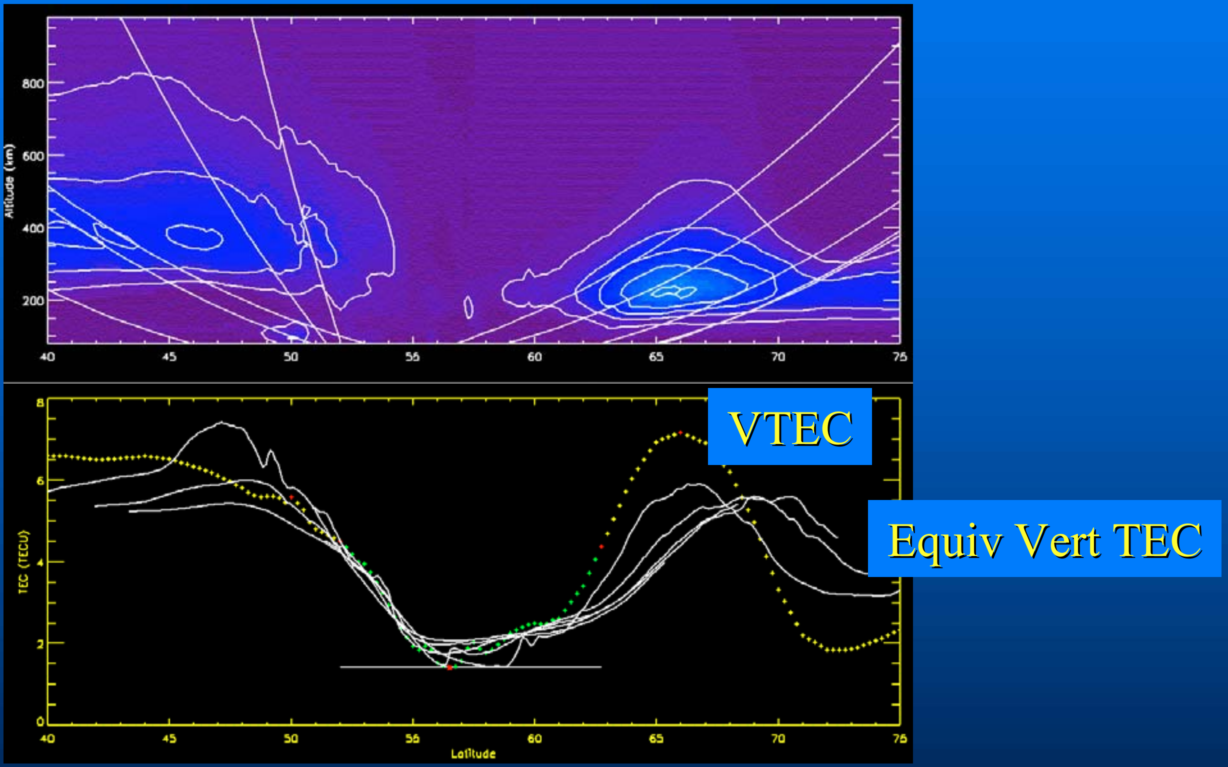

- In practice, all measurements limited to accuracy of a few TECU

Prifysgol Cymru Aberystwyth The University of Wales

Ionospheric Scintillation

Effects of small-scale irregularities in ionospheric electron density on transionospheric propagation

Scintillation – basic ideas

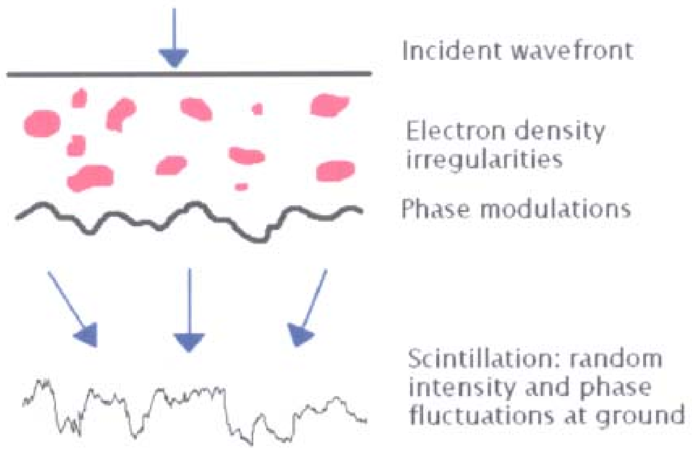

Figure 1. Schematic of mechanism of scintillation.

- diffraction pattern on ground
- satellite motion or irregularity motion
- random temporal fluctuations of received signal
- both phase and amplitude (intensity)
- intensity may fade below receiver margin
- phase shifts can cause signal loss

Irregularity Spectrum

- perturbations in electron density *(ΔN)*
- *spatial* spectrum of irregularities has *power-law* form

  $\Phi_{\Delta N}(k_x) \propto k_x^{-p_{1D}}$ where k_x is wave number and p_{1D} is 1-D spectral index
- for *isotropic* irregularities

  $\Phi_{\Delta N}(k_x, k_y, k_z) \propto K^{-p}$ where K is 3-D wave number and $p = p_{1D} + 2$
- range of wave numbers

  inner scale - set by diffusion processes - metres

  outer scale - ? - tens of km

Scintillation Spectra

- *temporal* spectra for weak scintillation
- *phase* (φ) fluctuations

$$\Phi_\varphi\ (\Omega) \propto \Omega^{-p_s} \quad \text{where } \Omega \text{ is fluctuation frequency and } p_s = p - 1$$

- *intensity* (I) fluctuations

$$\Phi_I\ (\Omega) \propto \Omega^{-p_s} \qquad \text{for} \quad \Omega >> \Omega_F$$

- Ω_F is *Fresnel frequency*

Fresnel cut-off

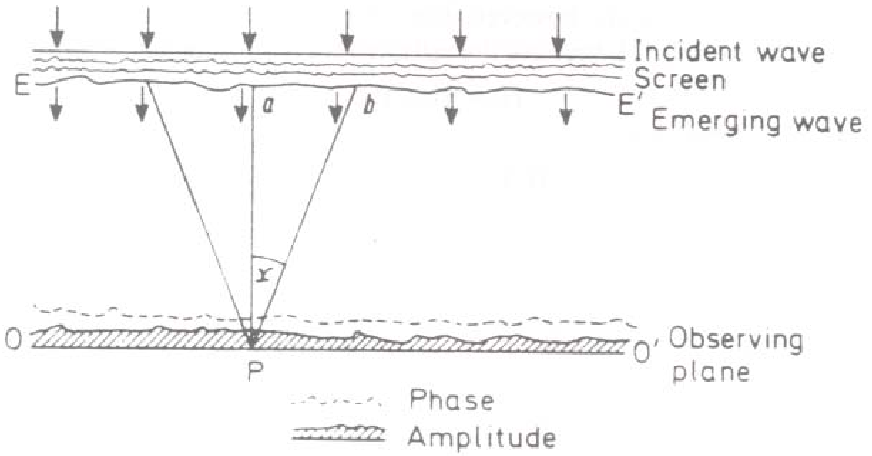

Fig. 2.10 Diffraction of a plane wave incident on a thin phase-changing screen.

- constructive interference for Pb < Pa + λ/2
- irregularities of Fresnel zone size will contribute most to amplitude (intensity) scintillation
- $r_F \sim \sqrt{(\lambda z)}$ where λ is radio wavelength and z is altitude of irregularities
- scintillation caused by sub-kilometre irregularities (eg GPS L1: *λ ~ 0.2 m, so for z ~ 350 km,* $r_F \sim 250$ *m*)

Prifysgol Cymru Aberystwyth The University of Wales

Spectra

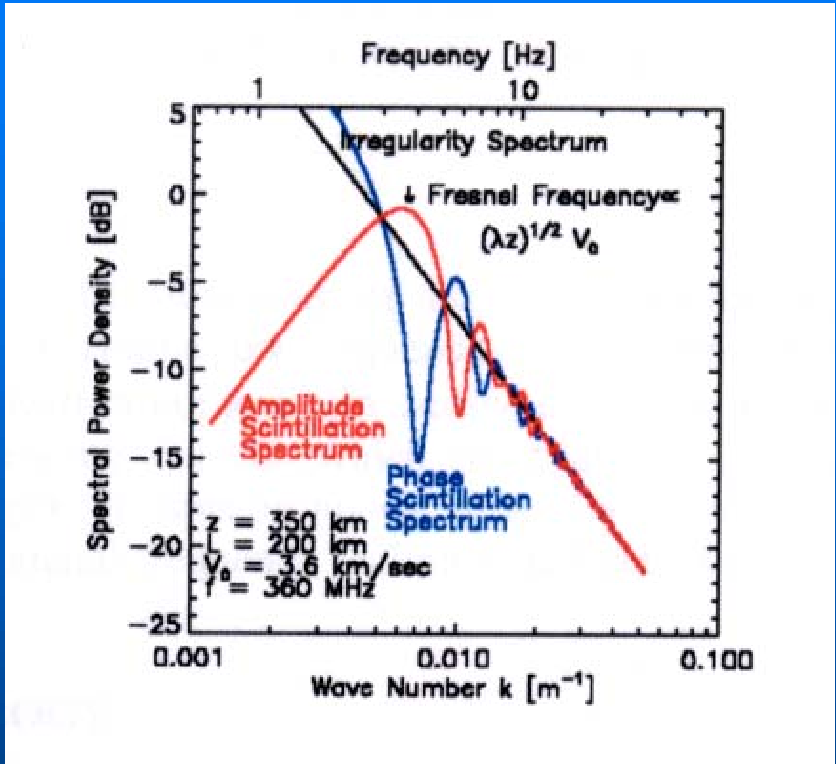

Theoretical (Wernik et al., 2003)

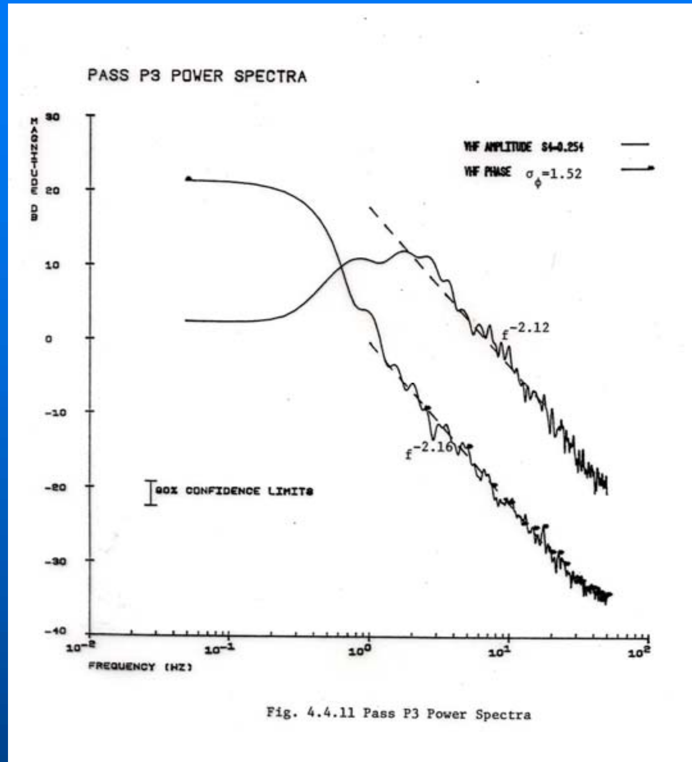

Experimental

Spectral index –spectral slope

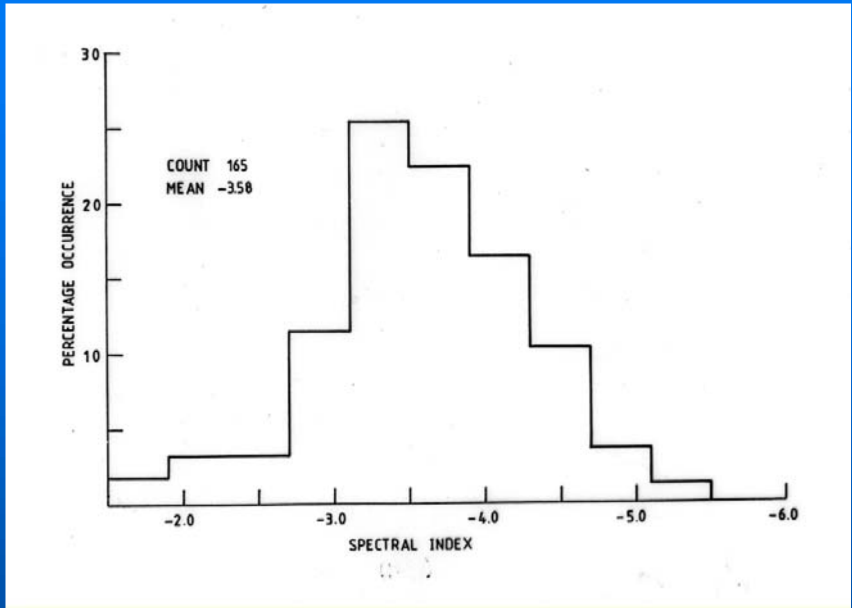

- range ~2 to ~5
- p_s often taken to be 3

Scintillation indices – measurements of scintillation

- Intensity fluctuations *(S_4)*

$$S_4 = \{ (< I^2 > - < I >^2) / < I >^2 \}^{1/2}$$

- Phase fluctuations *sigma phi (σ_φ)*

$$\sigma_\varphi = \{ < \varphi^2 > - < \varphi >^2 \}^{1/2}$$

  - in practice, signal processing involves filtering to remove effects of large-scale TEC structures
  - must specify de-trend cut-off used

- S_4 and σ_φ depend on
  - $< \Delta N^2 >$
  - irregularity anisotropy
  - propagation geometry

Prifysgol Cymru Aberystwyth The University of Wales

Scintillation Theory

Intensity

$$S_4^2 = r_e^2 \lambda^2 (L \sec\theta)\, C_s\, Z^{\nu-1/2} \cdot \left[\frac{\Gamma((2.5-\nu)/2)}{2\sqrt{\pi}\,\Gamma((\nu+0.5)/2)(\nu-0.5)}\right] \mathcal{J}$$

where

$$\mathcal{J} = \frac{ab}{\sqrt{A''C''^{\nu}}}\, {}_2F_1\left(\tfrac{1}{2}-\nu,\ \tfrac{1}{2};\ 1;\ \frac{A''-C''}{A''}\right)$$

S_4 depends on

- strength of irregularities *(C_s)*
- spectral slope *($p = 2\nu$)*
- irregularity shape
- propagation geometry (irregularities are field aligned)
- Fresnel zone size *(Z)*

Phase

$$\langle\delta\phi^2\rangle = r_e^2 \lambda^2 (L \sec\theta)\, G\, C_s \frac{q_0^{-2\nu+1}\,\Gamma(\nu-\tfrac{1}{2})}{4\pi\Gamma(\nu+\tfrac{1}{2})}$$

where

$$G = \frac{ab}{\sqrt{AC - B^2/4}\,\cos\theta}$$

σ_φ depends differently on

- strength of irregularities *(C_s)*
- spectral slope *($p = 2\nu$)*
- irregularity shape
- propagation geometry
- *but* not *Z*

Rino, C. L., *Radio Sci.*, 14, 1135, 1979.

Dependence on radio frequency

- Intensity scintillation

$$S_4 \propto f^{-(3+p_s)/4}$$

$$S_4 \sim f^{-1.5} \quad \text{for } p_s \sim 3$$

- Phase scintillation

$$\sigma_\varphi \sim f^{-1}$$

not limited by Fresnel zone size

Scintillations on various carrier frequencies

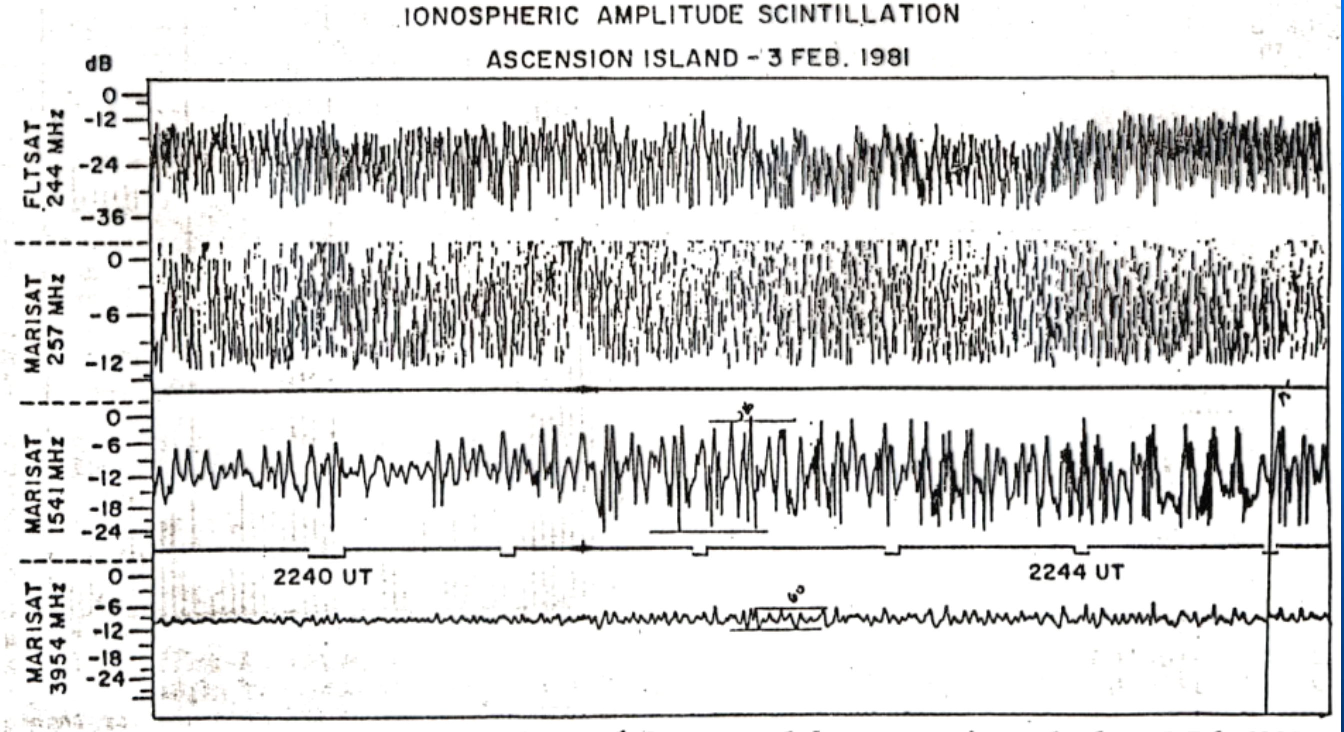

Fig. 4. Sample of UHF, L-band and C-band data recorded at Ascension Island on 3 Feb 1981. Both UHF and L-band show saturated scintillations and there is 6 dB scintillation at C-band.

Prifysgol Cymru Aberystwyth The University of Wales

Structure of scintillating signal

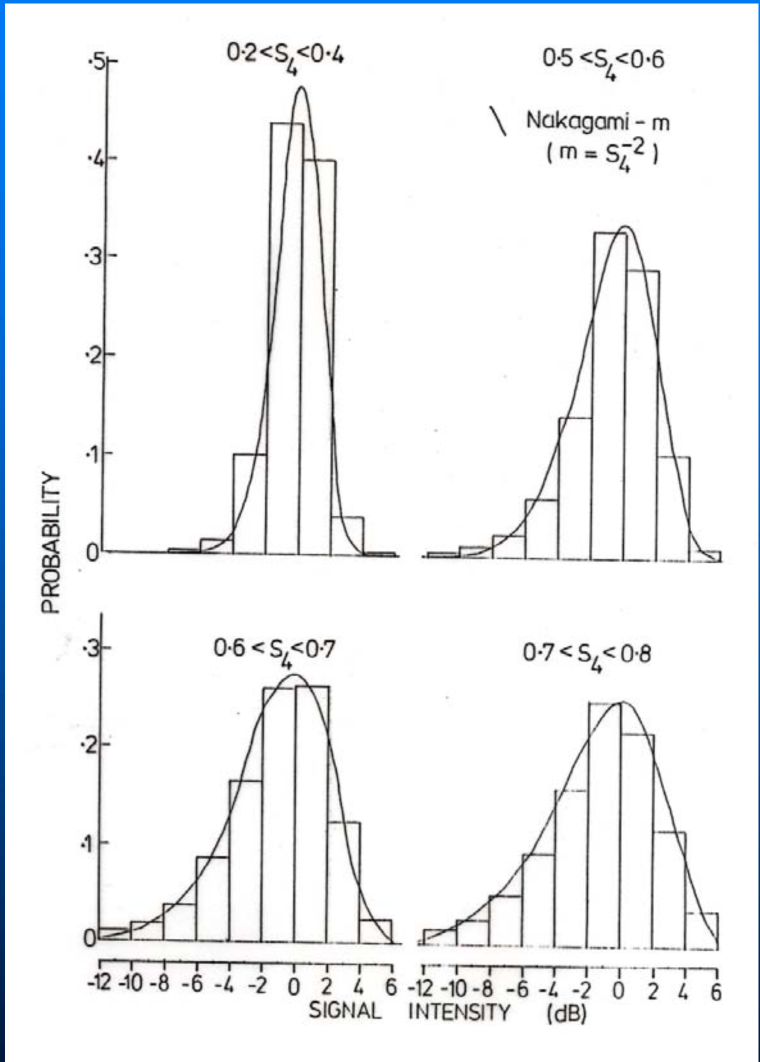

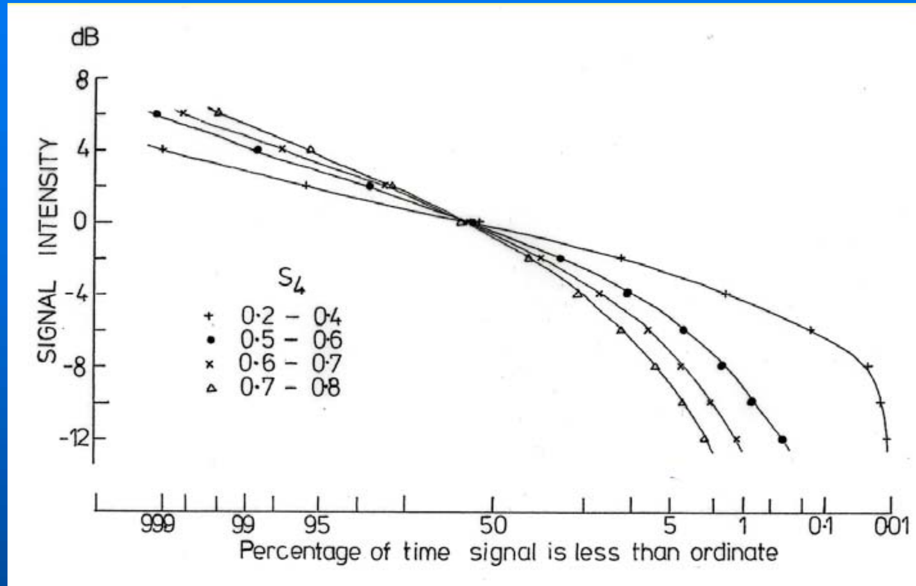

Depth of fading related to S_4

Irregularity anisotropies

Plasma constrained by magnetic field

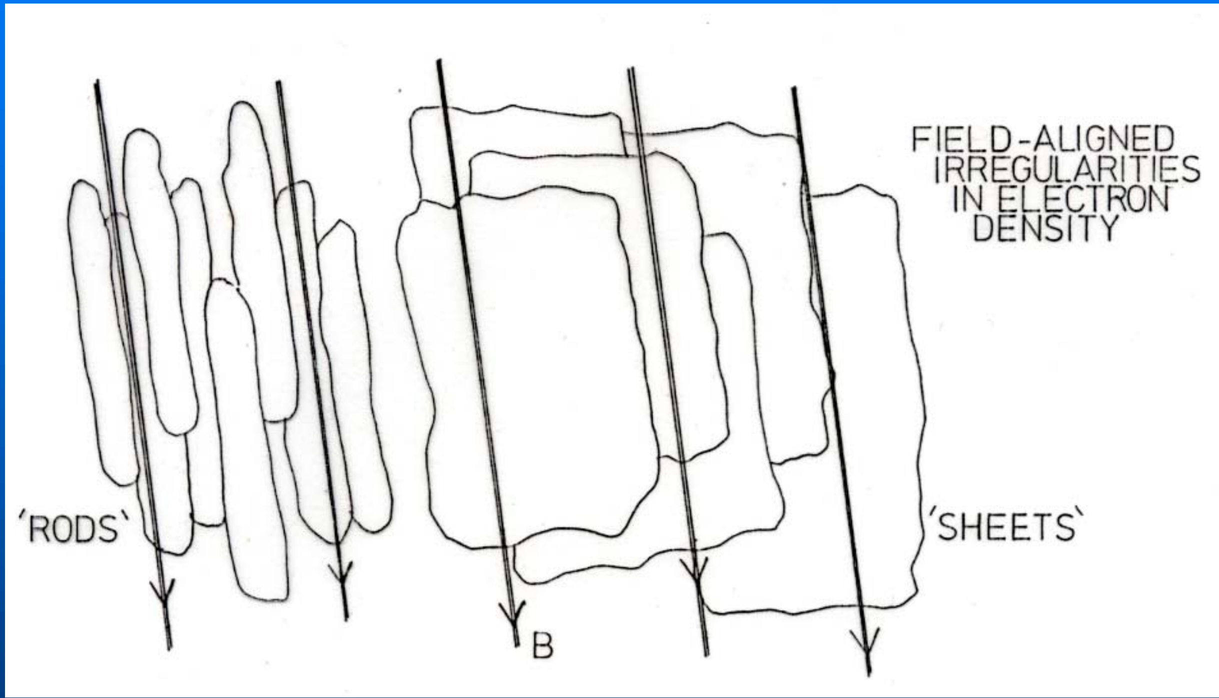

- field-aligned 'rods'
- axial ratio (x : 1 : 1)
- sub-auroral latitudes

- L-shell confined 'sheets'
- axial ratio (x : y : 1)
- auroral zone

Geometrical effects

Theoretical estimates for Kiruna as a function of latitude

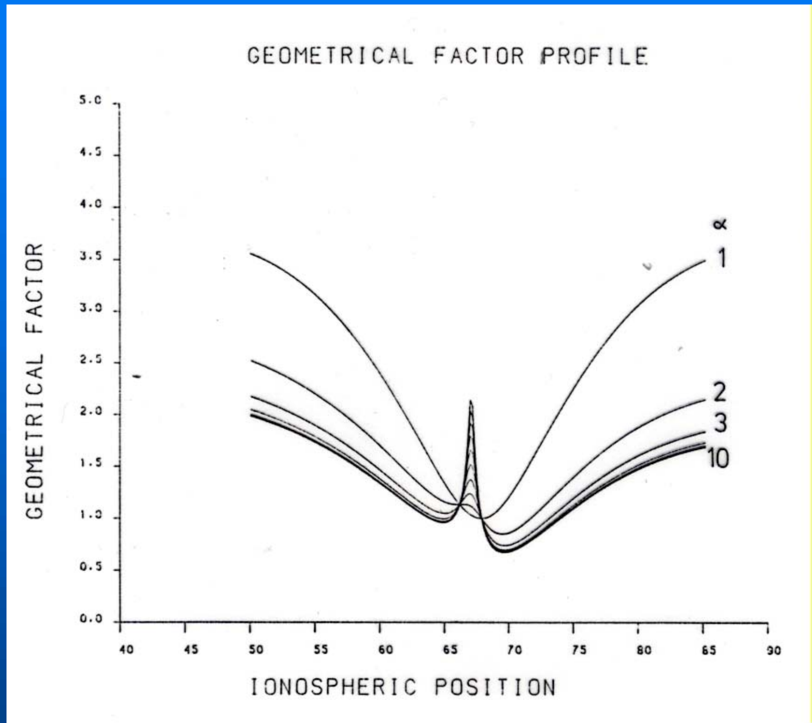

- multiplying factor normalised to overhead
- rod-like irregularities
- axial ratios up to $\alpha = 1 : 10$
- function of latitude

Geometrical effects on S_4

Experimental observations on 150 MHz at Lerwick – a *sub-auroral* station

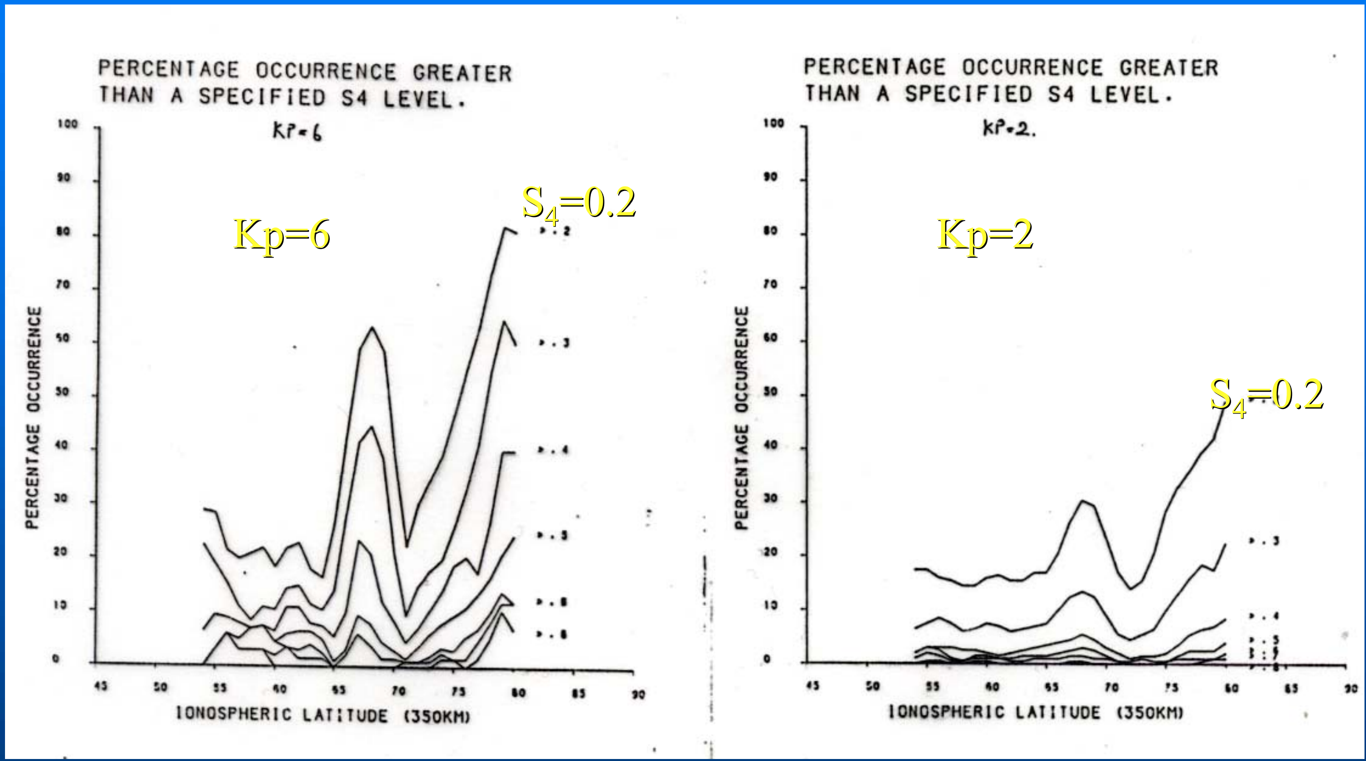

- enhancement looking up field line
- evidence for *rod-like* irregularities
- scintillation boundary
- irregularity zone moves equatorwards with Kp

Geometrical effects on S_4

Theoretical estimates for Kiruna as a function of azimuth

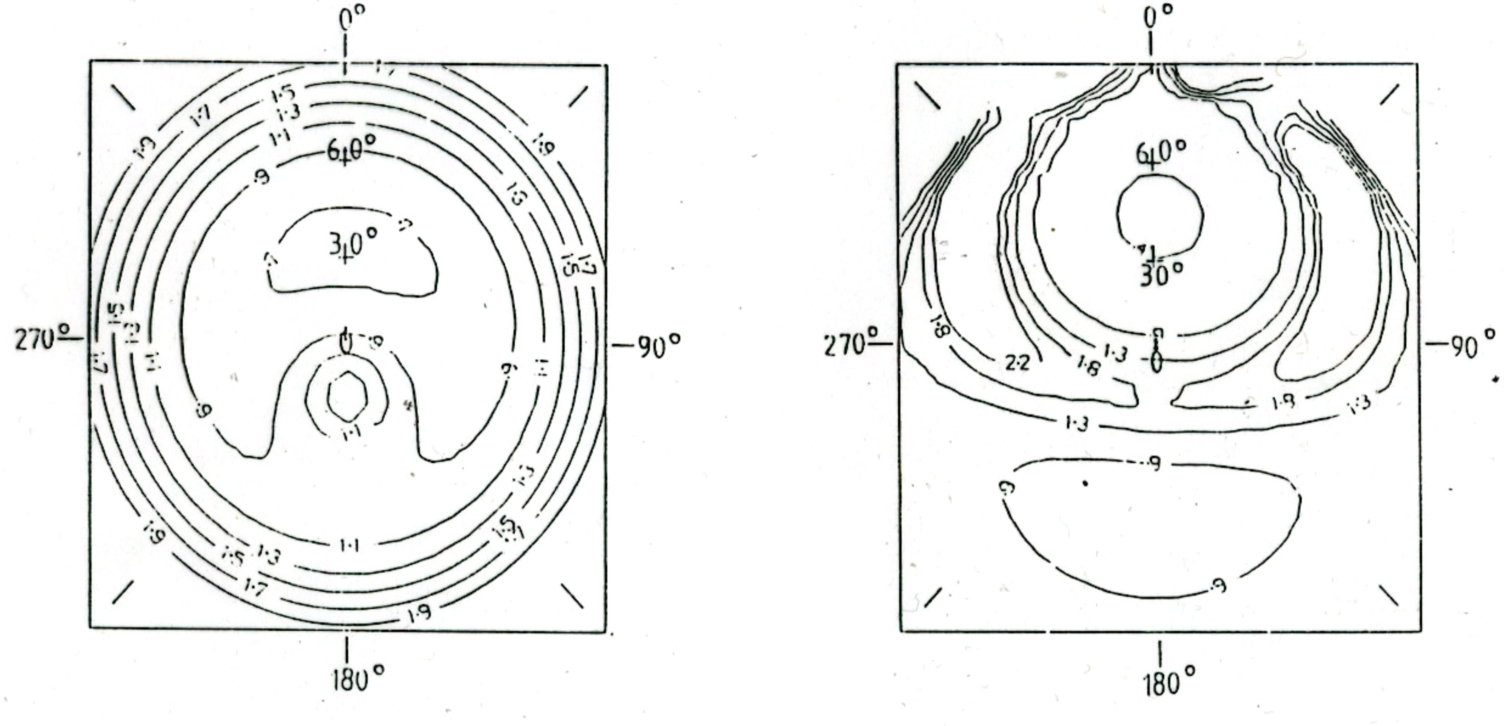

(a) field-aligned rods (5:1)

(b) L-shell confined sheets (5:5:1)

Figure 5 Plots of the geometrical multiplying factor in the modelled S_4 index as a function of azimuth and elevation.

- Field-aligned rods
- (5:1)

- L-shell confined sheets
- (5:5:1)

Geometrical effects on scintillation

Phase scintillation at Kiruna – an *auroral* zone station

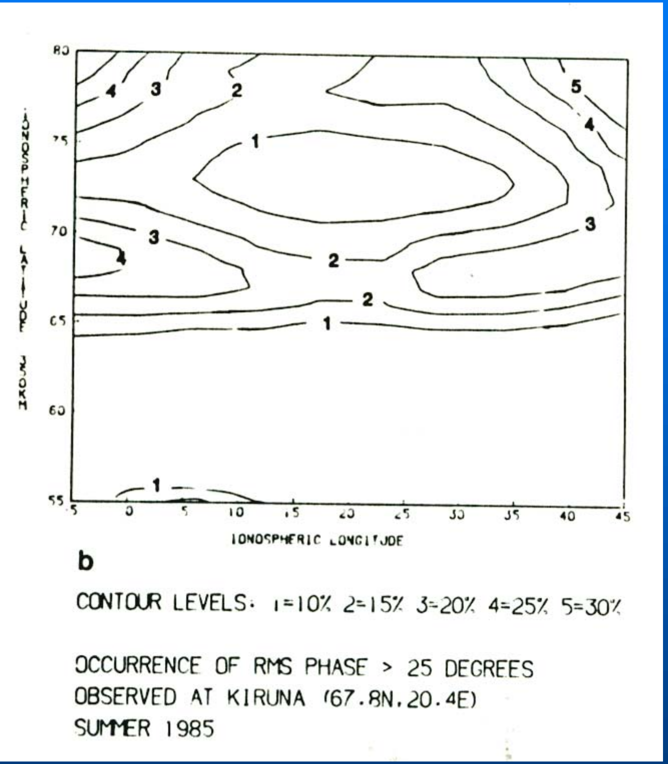

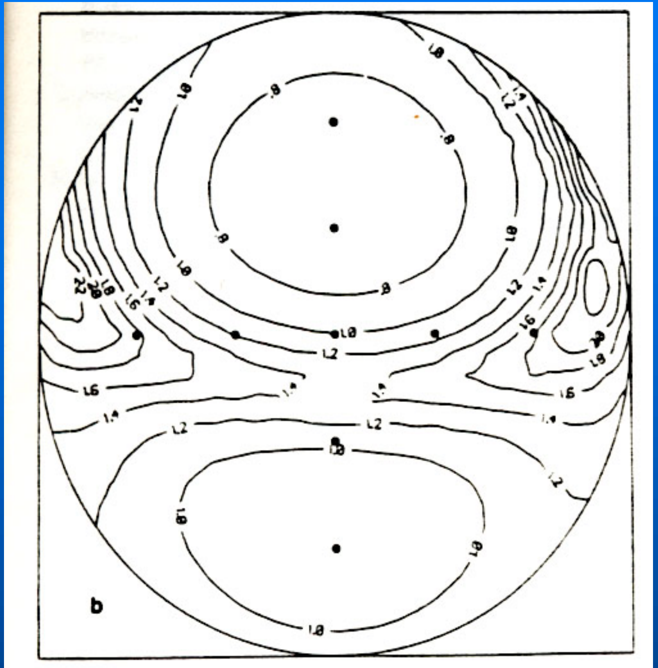

Fig. 8. Estimates of the geometrical factor in σ_φ normalized to overhead measurements.

- phase scintillation occurrence
- experimental results at 150MHz
- different propagation directions

- geometrical factor
- irregularity sheets (8:8:1)

- Evidence for sheet-like irregularities in auroral zone

Global scintillation morphology

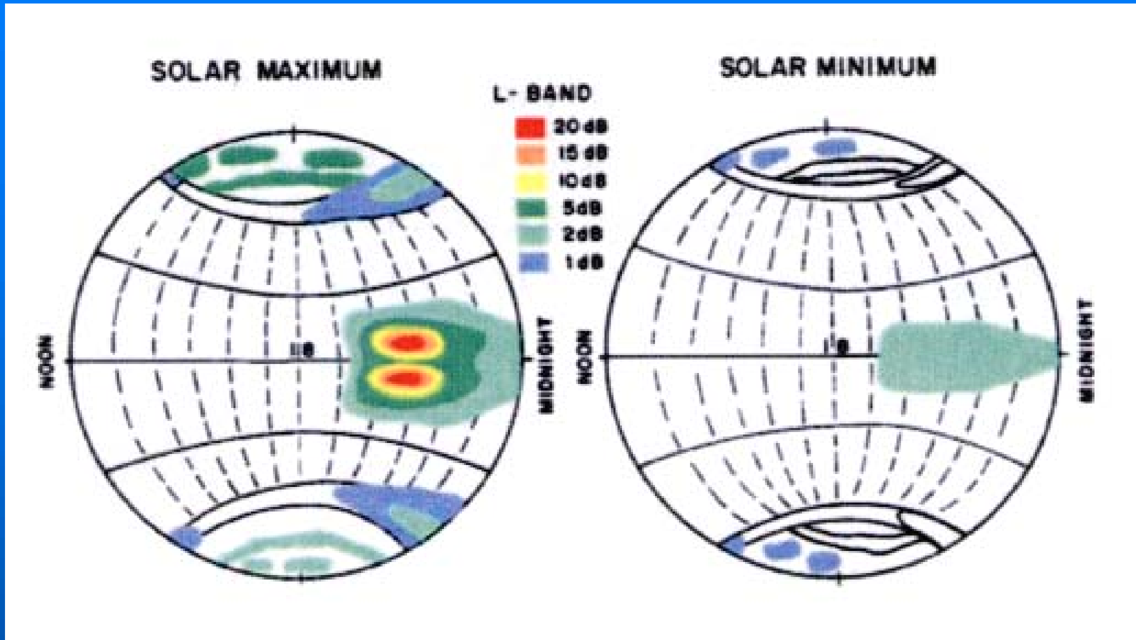

Figure 3. Global variation of scintillation fades during solar maximum and solar minimum conditions. Understanding of these patterns was developed in a series of apers over many years by Aarons, though the figure above has been taken from Basu et al. (1988).

- the most severe scintillation effects are found in the post-sunset equatorial ionosphere
- equatorial morphology is longitude dependent

Auroral scintillation

Kiruna 150 MHz

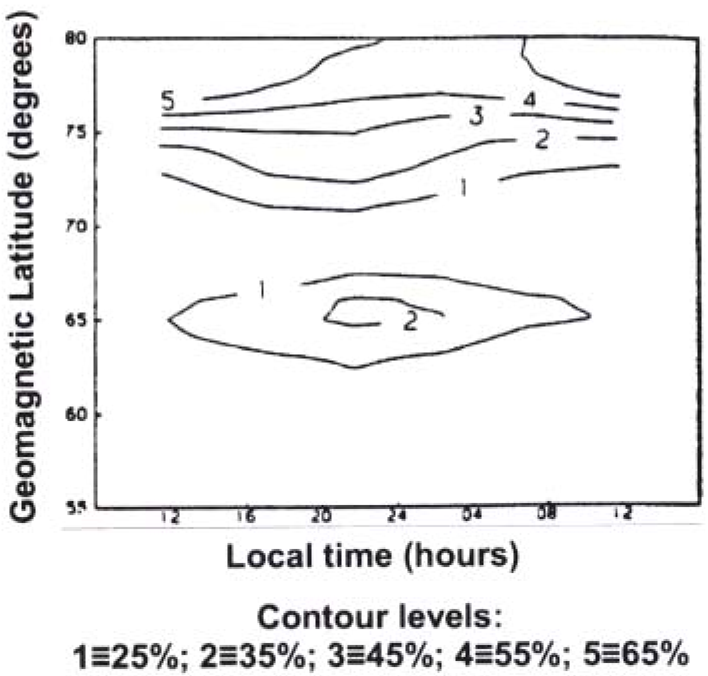

Figure 5. Diurnal variation of occurrence S_4>0.2 at Kiruna (64.3°CGM Lat, 102.8°CGM Lon) during winter 1985/1986 (after Kersley et al., 1988c).

- Nighttime maximum

Prifysgol Cymru
Aberystwyth
The University of Wales

Sub-auroral scintillation

Lerwick 150MHz

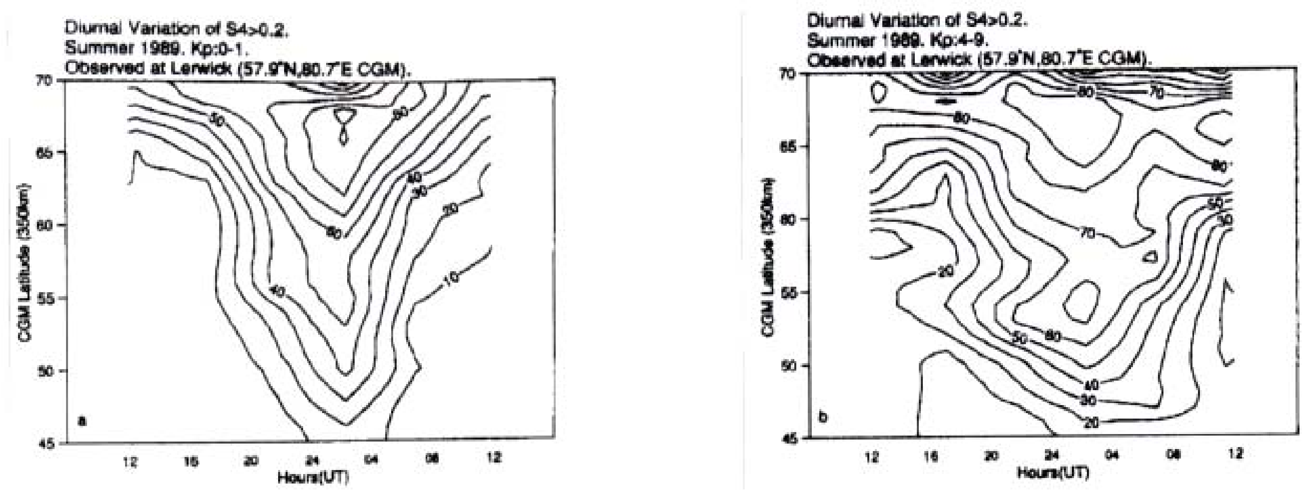

Figure 6: Diurnal variation of occurrence of S4>0.2 measured at Lerwick during summer 1989, under a) quiet and b) disturbed geomagnetic conditions (after Pryse et al., 1991).

- scintillation boundary
- evening equatorwards advance
- extension with geomagnetic disturbance

Prifysgol Cymru Aberystwyth The University of Wales

Auroral scintillation

Kiruna 150 MHz

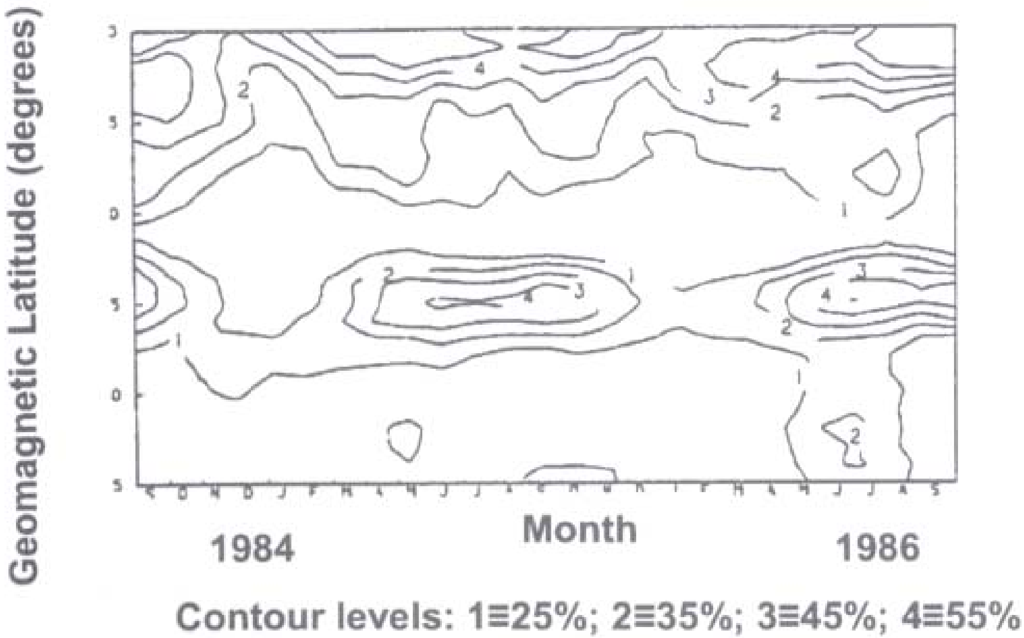

Figure 7. Occurrence of S4>0.2 measured at Kiruna between September 1984 and September 1986 (after Kersley et al., 1988c).

- summer maximum at solar minimum

Sub-auroral scintillation

Lerwick 150 MHz

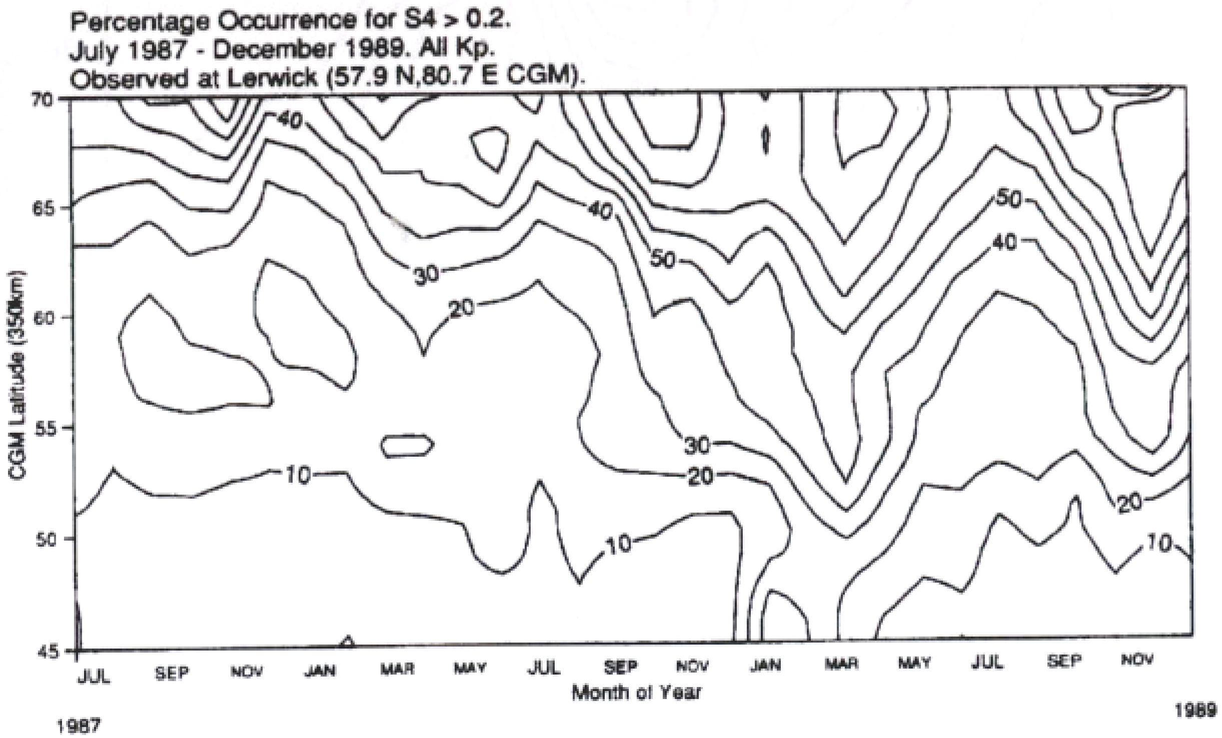

Figure 8. Occurrence of S_4>0.2 measured at Lerwick between July 1987 and November 1989 (after Pryse et al., 1991).

- equatorwards extension with rising solar activity

Polar-cap scintillation

Ny Alesund 150 MHz

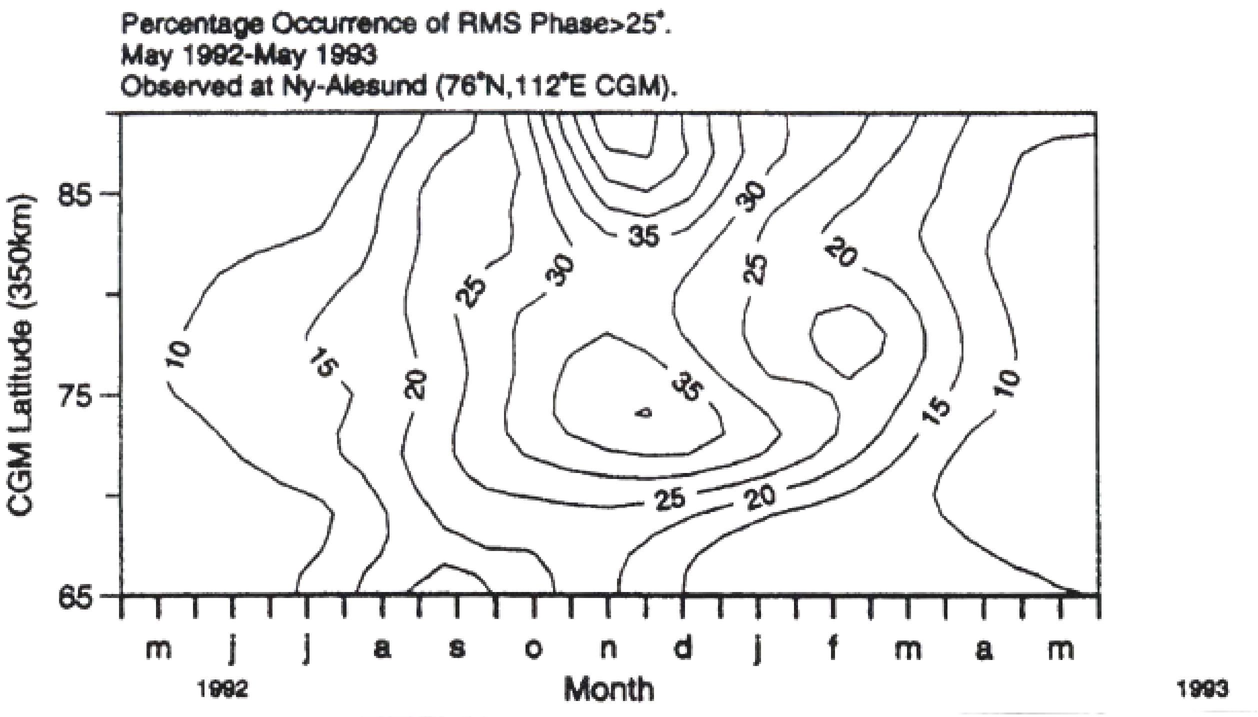

Figure 9. Occurrence of σ_φ>25°, measured at Ny Ålesund between March 1992 and March 1993 (after Kersley et al., 1995).

- winter maximum
- evidence for wing-like irregularities

Prifysgol Cymru Aberystwyth The University of Wales

Scintillation modelling and forecasting

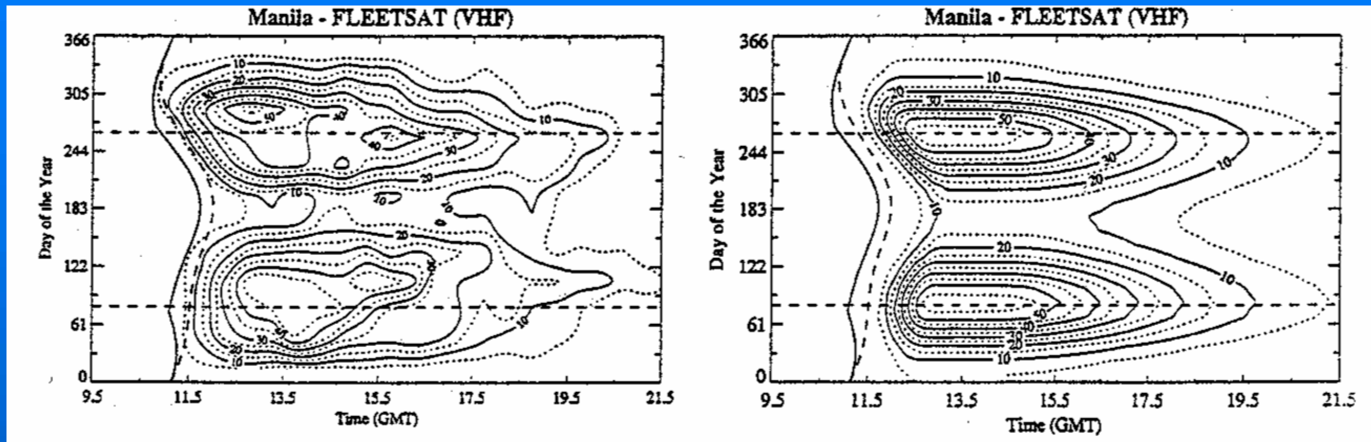

Figure 10. Percentage occurrence of S_4>0.5 for Manila: a) measured levels and b) modelled levels (after Secan et al., 1995). The heavy solid curves on the lhs indicate the time of E-region sunset and the heavy dashed curves the time of F_2 region sunset. The horizontal dashed lines indicate the equinoxes.

Scintillation models

- WBMOD
- GISM

Prifysgol Cymru Aberystwyth The University of Wales

Irregularity mechanisms

What causes the irregularities?

- Plasma instabilities
  - Equatorial scintillation
    - Rayleigh-Taylor gravitational instability
  - High-latitude scintillation
    - ExB gradient drift instability
    - velocity shears
- Soft-particle precipitation
  - Auroral scintillation
    - in-situ fine-structured

Prifysgol Cymru
Aberystwyth
The University of Wales

Transionospheric propagation - conclusions

- *Total electron content (TEC)* along ray path is a key parameter
- *Carrier phase, group delay and polarisation* of received signal are modified by crossing ionosphere
- *TEC* has *large temporal and spatial variability* on *many different scales*
- *Small-scale irregularities* in electron density cause *scintillation* of received signal
- *TEC and scintillation* introduce errors and cause problems for operation of *applied radio systems like GPS*

Prifysgol Cymru
Aberystwyth
The University of Wales